LIUTEX-BASED AND OTHER MATHEMATICAL, COMPUTATIONAL AND EXPERIMENTAL METHODS FOR TURBULENCE STRUCTURE

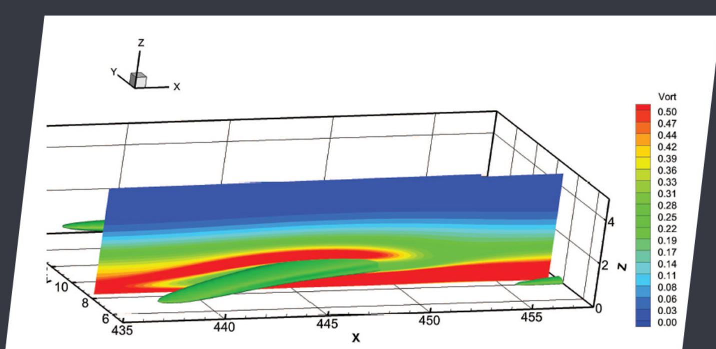

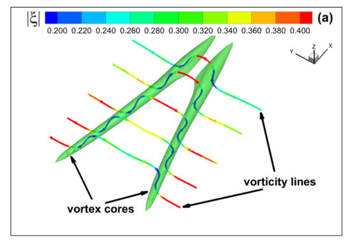

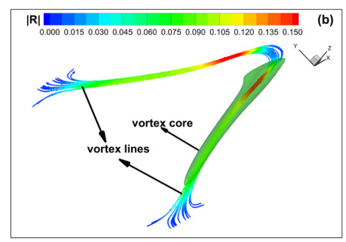

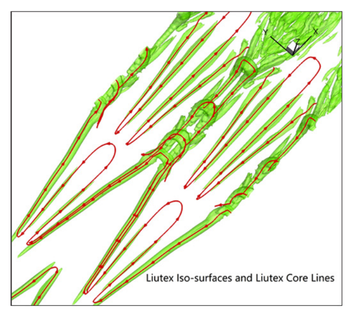

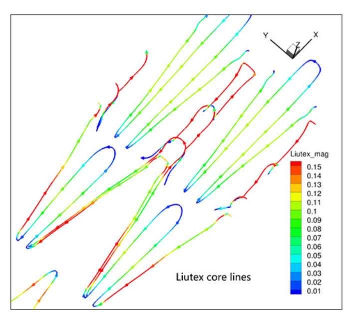

Editors:

Chaoqun Liu

Yisheng Gao

Bentham Books

Current Developments in Mathematical Sciences

(Volume 2)

Liutex-based and Other Mathematical, Computational and Experimental Methods for Turbulence Structure

Edited by

Chaoqun Liu
Department of Mathematics,
University of Texas at Arlington,
Arlington, Texas 76019,
USA

&

`Yisheng Gao
College of Aerospace Engineering,
Nanjing University of Aeronautics and Astronautics ,
Nanjing 210016,
China

Current Developments in Mathematical Sciences

Volume # 2

Liutex-based and Other Mathematical, Computational and Experimental Methods for Turbulence Structure

Editor: Chaoqun Liu & Yisheng Gao

ISSN (Online): 2589-272X

ISSN (Print): 2589-2711

ISBN (Online): 978-981-14-3760-1

ISBN (Print): 978-981-14-3758-8

ISBN (Paperback): 978-981-14-3759-5

Published by Bentham Science Publishers Pte. Ltd. Singapore.

need for a court order if at any point you breach any terms of this License Agreement. In no event will any delay or failure by Bentham Science Publishers in enforcing your compliance with this License Agreement constitute a waiver of any of its rights.

3. You acknowledge that you have read this License Agreement, and agree to be bound by its terms and conditions. To the extent that any other terms and conditions presented on any website of Bentham Science Publishers conflict with, or are inconsistent with, the terms and conditions set out in this License Agreement, you acknowledge that the terms and conditions set out in this License Agreement shall prevail.

Bentham Science Publishers Pte. Ltd.
80 Robinson Road #02-00
Singapore 068898
Singapore
Email: subscriptions@benthamscience.net

BENTHAM SCIENCE

CONTENTS

PREFACE

Turbulence is a centuries-long world puzzle. Turbulence coherent structure really means vortex structure. However, there was no mathematical definition of vortex ever before and there was no mathematical definition for turbulence either. Therefore, there was no vortex science or vortex dynamics since vortex had no definition. Since turbulence is built up and driven by vortices, there was no serious scientific research on turbulence theory and turbulence structure because there was no definition of vortex. This book collected a lot of scientific efforts to give an accurate and mathematical definition of vortex, that is Liutex developed by Liu *et al* [C. Liu *et al.*, Phys. Fluids **30**, 035104 (2018)].

The core of this book is a collection of papers presented in the 13th World Congress of Computational Mechanics (WCCM2018), Symposium 704, **Mathematics and Computations for Multiscale Structures of Turbulent and Other Complex Flows**, New York, United States on July 27, 2018. This book also collects quite a number of other research papers working on the vortex definition, vortex identification and turbulence structure from different insight angles including mathematics, computations and experiments. Of course, the priority is dedicated to an accurate and mathematical definition for vortex, which was first named “RORTEX” in 2018 and was changed to “LIUTEX” approved unanimously by alliance of six universities and Alliance of Vortex Research in 2019. Besides Liutex, this book also publishes a lot of efforts to do analysis on turbulence structure by unobjectionable mathematics, incredible DNS computations, and marvelous experiments.

This book contains thirteen chapters which are briefly introduced in this preface.

The first chapter, Liutex – A New Mathematical Definition of Vortex and Vorticity Decomposition for Turbulence Research, is written by Chaoqun Liu, Yisheng Gao and Yifei Yu at University of Texas at Arlington. For long time, people recognize vortex as vorticity tube and measure the vortex rotation strength by vorticity magnitude. These misunderstandings have been carried out by thousands of research papers and almost all textbooks. Robinson (1989) has found the association between regions of strong vorticity and actual vortices can be rather weak. Many vortex identification criteria have been proposed. However, vortex still has no rigorous mathematical definition with direction and magnitude and the relationship between vortex and vorticity was unknown. Because we do not have definition for vortex, there was really no vortex science. Since vortex is the building block and the muscle of turbulence, lack of mathematical definition for vortex becomes a bottle neck for turbulence research. Really, there was no serious turbulence research without definition of vortex. In our recent work, a mathematical definition called Liutex (Previously called Rortex) is given to identify the rigid rotation of fluid motion. Since vortex core is near the rigid rotation, Liutex naturally represents the vortex cores. Liutex is a local mathematical vector definition with direction and magnitude of pure rotation without shear contamination, which is unique and Galilean invariant. The Liutex direction is defined as the local rotation axis and the Liutex magnitude is the local rotation. More important, we derive the accurate mathematical relation between vorticity and vortex, which is Vorticity = Liutex + Antisymmetric Shear (RS decomposition). This new discovery is an important breakthrough in modern fluid dynamics and is extremely important for turbulence research. In addition, the velocity gradient tensor has been decomposed to two parts, R (rigid rotation) and NR (non-rotation part) as a counterpart of the traditional Cauchy-Stokes decomposition (Helmholtz decomposition) which is improper since vorticity cannot represent flow rotation. Liutex is a new physical quantity like velocity, vorticity, temperature, pressure, which has been ignored by our founding fathers of fluid dynamics for centuries but is particularly important for vortex dynamics and turbulence research. Introduction of Liutex, RS decomposition of vorticity, and R-NR decomposition of velocity gradient would open a new era for vortex dynamics and new turbulence research, likely new fluid dynamics.

The second chapter, Liutex – a New Vortex definition, and its Calculation and Galilean Invariance, is written by Yiqian Wang, Yisheng Gao and Chaoqun Liu from University of Shanghai for Science and Technology in China and University of Texas at Arlington in USA. The Liutex (previously known Rortex) method introduces a vortex vector field to mathematically and systematically describe vortices in flow fields. In the present study, the calculation procedure of Liutex is revisited which includes two-step reference coordinate rotation. Then, for the first time, an explicit formula to calculate Liutex is derived and the physical intuition and efficiency improvement brought by this formula are discussed. In addition, the Galilean invariance, which has been widely accepted as a preliminary check for a successful vortex identification method is discussed for Liutex vector.

The third chapter, New Omega Vortex Identification Method Based on Determined Epsilon, is authored by Xiangrui Dong, Yisheng Gao, Chaoqun Liu from University of Shanghai for Science and Technology and University of Texas at Arlington. A new Omega method with ε determination is introduced to represent the ratio of vorticity square over the sum of vorticity square and deformation square, for the vortex identification. the advantages of the new Ω method can be summarized as follows: (1) Omega, as a ratio of the vorticity squared over the sum of the vorticity squared and deformation squared, is a normalized and case-independent function which satisfies $\Omega \in [0,1]$; (2) Compared with the other vortex visualization methods, which require a wide threshold change to capture the vortex structures, Ω can always be set as 0.52 to capture vortex for different cases and time steps; (3) ε is defined as a function without any adjustment on its coefficient in all cases; (4) The Ω method can capture both strong and weak vortices simultaneously. In addition, Ω method is quite robust with no obvious change in vortex visualization.

The fourth chapter, Stability Analysis on Shear Flow and Vortices in Late Boundary Layer Transition, is solely authored by Jie Tang from University of Texas at Arlington. Turbulence is still an unsolved scientific problem, which has been regarded as "the most important unsolved problem of classical physics". Liu proposed a new mechanism about turbulence generation and sustenance after decades of research on turbulence and transition. One of them is the transitional flow instability. Liu believes that inside the flow field, shear (dominant in laminar) is unstable while rotation (dominant in turbulence) is relative stable. This inherent property of flow creates the trend that non-rotational vorticity must transfer to rotational vorticity and causes the flow transition. To verify this new idea, this chapter analyzed the linear stability on two-dimensional shear flow and quasi-rotational flow. Chebyshev collocation spectral method is applied to solve Orr–Sommerfeld equation. Several typical parallel shear flows are tested as the basic-state flows in the equation. The instability of shear flow is demonstrated by the existence of positive eigenvalues associated with disturbance modes (eigenfunctions), *i.e.* the growth of these linear modes. Quasi-rotation flow is considered under cylindrical coordinates. An eigenvalue perturbation equation is derived to study the stability problem with symmetric flows. Shifted Chebyshev polynomial with Gauss collocation points is used to solve the equation. To investigate the stability of vortices in flow transition, a ring-like vortex and a leg-like vortex over time from our Direct Numerical Simulation (DNS) data are tracked. The result shows that, with the development over time, both ring-like vortex and leg-like vortex become more stable as Omega becomes close to 1.

The fifth chapter, POD and DMD Analysis in Late Flow Transition with Omega Method, is authored by Sita Charkrit and Chaoqun Liu at Department of Mathematics, University of Texas at Arlington, Arlington, Texas 76019, USA. In this chapter, the proper orthogonal decomposition (POD) and dynamic mode decomposition (DMD) are applied to analyze the 3D late transitional flow on the flat plate obtained from Direct numerical simulation (DNS). POD is used to find the most persistent spatial structures while DMD is used to find single frequency modes. The omega method is applied as a vortex identification to visualize vortices with iso-surfaces $\Omega = 0.52$. The results in POD and DMD are discussed and compared to show the same and different features such as shapes, amplitudes and time evolutions.

The sixth chapter, Comparison of Liutex and Eigenvalue-based Vortex Identification Criteria for Compressible Flows, is written by Yisheng Gao and Chaoqun Liu at Department of Mathematics, University of Texas at Arlington, Arlington, Texas 76019, USA. Most of the currently popular vortex identification methods, including the $\mathbf{Q}$ criterion, the Δ criterion and the $\boldsymbol{\lambda}_{\mathbf{ci}}$ criterion, are exclusively determined by the eigenvalues or invariants of the velocity gradient tensor and thereby can be classified as eigenvalue-based criteria. However, these criteria will suffer from several shortcomings, such as inadequacy of identifying the rotational axis and contamination by shearing. Recently, a new eigenvector-based Liutex method (previously named Rortex) was proposed to overcome the issues associated with the eigenvalue-based criteria. In this paper, the comparison of Liutex and two eigenvalue-based criteria, namely the $\boldsymbol{\lambda}_{\mathbf{ci}}$ criterion and a modification of the original $\mathbf{Q}$ criterion, are performed to assess these methods for compressible flows. According to the analysis of the deviatoric part of the local velocity gradient tensor, all the scalar, vector and tensor forms of Liutex are valid for compressible flows without any modification, while two eigenvalue-based criteria, though applicable to compressible flows, are prone to severe contamination by shearing as in incompressible flows. Vortex structures in the problem of shock-vortex interaction are examined to confirm the validity and superiority of Liutex in compressible flows.

The seventh chapter, Observation of Coherent Structures of Low Reynolds Number Turbulent Boundary Layer by DNS and Experiment, is written by Panpan Yan from Beijing Jiaotong University, Beijing, 100044, China, Chaoqun Liu from University of Texas at Arlington, Yanang Guo and Xiaoshu Cai from University of Shanghai for Science and Technology, Shanghai, 200093, China. In order to study the characteristics of coherent structures of the turbulent boundary layer, the motion single frame, and long exposure imaging (MSFLE) method is proposed and an elaborate direct numerical simulation experiment was also conducted. MSFLE method is a Lagrangian measurement method, the speed of the camera is kept the same as the speed of the coherent structure, and the particle trajectory was captured by long exposure. By calculating the trace of the points on a chosen plane of the DNS result, we can obtain the particle trajectory like MSFLE method. Multilayer of vortex structures was observed and the evolution of the vortex packets with time was recorded.The result of the DNS simulation agrees well with the experiment. The size of the vortex of the different layer is almost the same, and no vortex breakdown was observed. The formation of the small-scale vortex is caused by sweeps and ejections of the larger coherent structures rather than the breakdown process.

The eighth chapter, Direct Numerical Simulation of Incompressible Flow in a Channel with Rib Structures, is authored by Ting Yu, Duo Wang, Heng Li and Hongyi Xu from Aeronautics and

Astronautics Department, Fudan University Shanghai PR China. The paper applied the state-of-the-art flow simulation method, i.e. the Direct Numerical Simulation (DNS), and strongly coupled the DNS with the heat-transfer governing equation to solve the thermal-turbulence problem in both 2-dimensional(2D) and 3-dimensional(3D) channel with rib tabulator structures. An innovative approach was applied to the simulations in one case. The surface roughness effects of the cooling vane were considered by including the roughness geometry in the DNS and the immersed-boundary method were invented to handle the geometry complexities due to the roughness. Two inlet conditions, namely the uniform flow and full-developed turbulence, were applied at the inflow surface of the channel. Half height of the channel was used as the scale length. The Prandtl number was set at Pr = 0.7. Five Reynolds number of 1000, 2500, 5000, 7500 and 1000 were calculated in the 2D cases and the Reynolds numbers of 2500 and 5000 were applied in 3D cases where a periodical condition was applied in the span-wise direction. Additionally, Reynolds number of 10000 was set in the case with roughened surface. The stream-wise velocity, turbulence intensity, the Nusselt (Nu) number were analyzed. Results in 2D cases and 3D cases presented a great difference on flow structure. At the same time, with increasing Reynolds number, the length of recirculation zone and the enhancement of heat transfer showed a decreasing trend. A vortex identification method, the newly-defined Rortex, was applied.

The ninth chapter, Vortex and Turbulent Structure Inside Hydroturbines, is written by Yuning Zhang from Key Laboratory of Condition Monitoring and Control for Power Plant Equipment (Ministry of Education), School of Energy, Power and Mechanical Engineering, North China Electric Power University, Beijing, China and Yuning Zhang from College of Mechanical and Transportation Engineering, China University of Petroleum-Beijing, Beijing China and Beijing Key Laboratory of Process Fluid Filtration and Separation, China University of Petroleum-Beijing, Beijing China. In this chapter, various kinds of vortex in the hydroturbines are briefly introduced with a focus on the swirling vortex rope in Francis turbine and the vortex in the vaneless space of the reversible pump turbine. The vortex induced pressure fluctuation and vibrations are initially demonstrated based on the on-site measurement in the power stations. Then, detailed characteristics of the vortex in the hydroturbines are demonstrated based on the plenty of examples together with the aid of the quantitative analysis.

The tenth chapter, Comparative Study of Supersonic Turbulent Channel flows between Thermally and Calorically Perfect Gases, is written by Xiaoping Chen from National-Provincial Joint Engineering Laboratory for Fluid Transmission System Technology, Zhejiang Sci-Tech University, Hangzhou, Zhejiang, China. In this chapter, to study the effects of gas model on the turbulent statistics and flow structures, direct numerical simulations (DNSs) of supersonic turbulent channel flow for thermally perfect gas and calorically perfect gas are conducted at Mach number 3.0 and Reynolds number 4800 combined with two wall temperature of 298.15K (low temperature condition) and 596.30 K (high temperature condition). The results show that, for high temperature condition, the effects of thermally perfect gas are important because the vibrational energy excited degree exceeds 0.1. Many of turbulent statistics used to express low temperature condition for calorically perfect gas still can be generalized for high temperature condition. The gas model does not have a significant influence on the strong Reynolds analogy. Omega could capture both strong and weak vortices simultaneously for supersonic flows, even under thermally perfect gas, which is difficult to obtain by Q. Compared to the results of calorically perfect gas, the vortex structure becomes smaller, sharper and more chaotic by considering thermally perfect gas.

The eleventh chapter The Experimental Study on Vortex Structures in Low Reynolds Number Turbulent Boundary Layer, was authored by Yanang Guo, Xiaoshu Cai, Wu Zhou, Lei Zhou, Xiangrui Dong from Institute of Particle and Two-phase Flow Measurement, University of Shanghai for Science and Technology, Shanghai, China. A motion single frame and long exposure (MSFLE) imaging method, which is a Lagrangian-type measurement, is experimentally carried out to study the vortex structures in a fully developed turbulent boundary layer with a low Reynolds number on a flat plate. In order to give the process of the vortex generation and evolution, on the one hand, the measurement system moves at the substantially same velocity as the vortex structure; on the other hand, a long exposure time is selected for recording the paths of the particles. In the experiment, the vortex structure characteristics as well as the temporal-spatial development can be shown by the streamwise-normal and streamwise-spanwise images which are extracted from a fully developed turbulent boundary layer. The result shows that the interaction between high and low-speed streaks induces the generation, deformation and 'breakdown' of the vortex structures, and badly influences the vortex evolution.

The twelfth chapter, Experimental Studies on Coherent Structures in Jet Flows using Single-Frame-Long-Exposure (SFLE) Method is authored by Lei Zhou, Xiaoshu Cai, Wu Zhou and Yiqian Wang from Institute of Particle and Two-phase Flow Measurement, University of Shanghai for Science, China. An experimental investigation on the flow structures in jet entrainment boundary layer flows based on the Single-Frame-Long Exposure (SFLE) method is carefully performed. It is found that two entrainment mode of 'engulfing' and 'nibbling' alternatively appear in the region of $2d$ to $3.5d$ in the axial direction and $1d$ to $1.25d$ in the radial direction with d being the diameter of jet nozzle. The appearance probability of such a pattern and the proportion of the 'engulfing' mode increases with Reynolds number Re when $Re \geq 1981$ (the Reynolds number is based on the nozzle diameter and jet velocity). However, the influence of Reynolds number on this flow pattern becomes weaker when $Re > 2245$. The main frequency of this structure is found to be between 10-19Hz with Fourier analysis. The vortical structures are further explored with the moving SFLE (MSFLE) method, and it is found that vortices always exist near the turbulent and non-turbulent interface (TNTI).

The last chapter (thirteenth), Hybrid Compact-WENO Scheme for the Interaction of Shock Wave and Boundary Layer, is co-authored by Jianming Liu from Jiangsu Normal University of China and Chaoqun Liu from Department of Mathematics, University of Texas at Arlington, Arlington, USA. In this chapter, an introduction on hybrid Weighted Essentially non-oscillatory (WENO) method is given. The hybrid techniques including both central and compact finite difference schemes are introduced. The paper reviews the driven mechanism of the high order finite scheme required for compressible flow with shock. The detailed constructing processes of the compact and WENO schemes are given and the hybrid detector.

I hope this book will be useful to scientists and engineers who are interested in fundamental fluid dynamics, vortex science and turbulence research.

In conclusion, I want to thank the numerous authors for their incredible contributions and having patience in assisting us. Furthermore, I want to acknowledge and thank the referees for their tiresome work on making this book come to fruition. Last but not the least, I would also like to thank my family including Weilan Jin (my wife), Haiyan Liu (my daughter) and Haifeng Liu (my

son) for their unconditional support. The co-editor, Yisheng Gao is also grateful to his family for the strong support.

Chaoqun Liu
Department of Mathematics,
University of Texas at Arlington,
Arlington, Texas 76019,
USA

List of Contributors

Chaoqun Liu	Department of Mathematics, University of Texas at Arlington, Arlington, Texas 76019, USA
Duo Wang	Department of Aeronautics and Astronautics, Fudan University, Shanghai, PR China
Heng Li	Department of Aeronautics and Astronautics, Fudan University, Shanghai, PR China
Hongyi Xu	Department of Aeronautics and Astronautics, Fudan University, Shanghai, PR China
Jianming Liu	School of Mathematics and Statistics, Jiangsu Normal University, Xuzhou 221116, China
Jie Tang	Department of Mathematics, University of Texas at Arlington, Arlington, Texas 76019, USA
Lei Zhou	Institute of Particle and Two-phase Flow Measurement, University of Shanghai for Science and Technology, Shanghai 200093, China
Panpan Yan	Shenyang Aircraft Design and Research Institute, Aviation Industry of China, Shenyang, 110035, China
Sita Charkrit	Department of Mathematics, University of Texas at Arlington, Arlington, Texas 76019, USA
Ting Yu	Department of Aeronautics and Astronautics, Fudan University, Shanghai, PR China
Xiaoshu Cai	Institute of Particle and Two-phase Flow Measurement, College of Energy and Power Engineering, University of Shanghai for Science and Technology, Shanghai 200093, China
Xiaoping Chen	National-Provincial Joint Engineering Laboratory for Fluid Transmission System Technology, Zhejiang Sci-Tech University, Hangzhou, Zhejiang 310018, China
Xiangrui Dong	Institute of Energy and Power Engineering, University of Shanghai for Science and Technology, Shanghai, China
Yisheng Gao	College of Aerospace Engineering, Nanjing University of Aeronautics and Astronautics, Nanjing 210016, China

Yanang Guo	Institute of Particle and Two-phase Flow Measurement, University of Shanghai for Science and Technology, Shanghai, China
Yiqian Wang	School of Mathematical Science, Soochow University, Suzhou 215006, China
Yifei Yu	Department of Mathematics, University of Texas at Arlington, Arlington, Texas 76019, USA
Yuning Zhang	Key Laboratory of Condition Monitoring and Control for Power Plant Equipment (Ministry of Education), School of Energy, Power and Mechanical Engineering, North China Electric Power University, Beijing 102249, China
Yuning Zhang	College of Mechanical and Transportation Engineering, China University of Petroleum-Beijing, Beijing 102249, China
Wu Zhou	Institute of Particle and Two-phase Flow Measurement, University of Shanghai for Science and Technology, Shanghai, China and School of Aerospace Engineering, Tsinghua University, Beijing, China

CHAPTER 1

Liutex – A New Mathematical Definition of Vortex and Vorticity Decomposition for Turbulence Research

Chaoqun Liu[1,*], Yisheng Gao[2] and Yifei Yu[1]

[1]*Department of Mathematics, University of Texas at Arlington, Arlington, Texas 76019, USA*

[2] *College of Aerospace Engineering, Nanjing University of Aeronautics and Astronautics, Nanjing 210016, China*

Abstract: For a long time, people recognize a vortex as a vorticity tube and measure the vortex rotation strength by vorticity magnitude. These misunderstandings have been carried out by thousands of research papers and almost all textbooks. It has been found that the association between regions of strong vorticity and actual vortices can be rather weak. Accordingly, many vortex identification criteria have been proposed. However, the vortex still has no rigorous mathematical definition and the relationship between the vortex and the vorticity is still not clear. Because we do not have a definition for the vortex, there exists no vortex science. Since the vortex is the building block and the muscle of turbulence, the lack of the mathematical definition for the vortex becomes a bottleneck for turbulence research. Actually, there is no serious turbulence research without the definition of the vortex. In our recent work, a mathematical definition called Liutex (previously called Rortex) is introduced to identify the rigid rotation of fluid motion. Liutex is a local mathematical vector definition with the direction and magnitude of pure rotation without shear contamination, which is unique and Galilean invariant. The Liutex direction is defined as the local rotation axis and the Liutex magnitude is the local rotation strength. More importantly, we derive the accurate mathematical relation between the vorticity and the vortex, which is Vorticity= Liutex + Antisymmetric Shear (RS decomposition). This new discovery is an important breakthrough in modern fluid dynamics and is extremely important for turbulence research. In addition, the velocity gradient tensor has been decomposed to two parts, R (rigid rotation) and NR (non-rotation part) as a counterpart of the traditional Cauchy-Stokes decomposition which is improper since the vorticity cannot represent flow rotation. Liutex is a new physical quantity like velocity, vorticity, temperature, pressure, which has been ignored by our founding fathers of fluid dynamics for centuries but is particularly important for vortex dynamics and turbulence research. The introduction of Liutex, RS decomposition of vorticity, and R-NR decomposition of the velocity gradient tensor would open a new era for vortex dynamics and new turbulence research, likely new fluid dynamics.

***Corresponding author Chaoqun Liu:** Department of Mathematics, University of Texas at Arlington, Arlington, Texas 76019, USA; Tel: +1-8172725151; Fax: +1-8172725802; E-mail: cliu@uta.edu

Keywords: Angular velocity, Coherent structures, Liutex, Turbulence, Velocity gradient tensor, Vortex identification, Vortex.

INTRODUCTION

Vortex is intuitively recognized as the rotational/swirling motion of the fluids. However, a universally accepted definition for vortex is yet to be achieved, which is probably one of the major obstacles causing considerable confusions and misunderstandings in turbulence research. Vorticity is mathematically defined as the curl of velocity. Vortices are ubiquitous in nature. As addressed by Küchemann "vortices are the sinews and muscles of turbulence" [1], some vortical structures, such as hairpin vortices, referred to as coherent turbulent structures [2], are recognized as one of the most important characteristics of turbulent flow and have been studied for more than 60 years [3]. It is generally acknowledged that intuitively, vortices represent the rotational/swirling motion of the fluids. However, a precise and rational definition of vortex is deceptively complicated and remains an open issue [4-5]. The lack of a consensus on the vortex definition has caused considerable confusions in visualizing and understanding the vortical structures, their evolution, and the interaction in complex vortical flows, especially in turbulence [4].

In classical vortex dynamics [4, 6-7], the vortex is usually associated with the vorticity which has a rigorous mathematical definition (the curl of velocity). Wu *et al.*, [4] define a vortex as "a connected region with high concentration of vorticity compared with its surrounding." Lamb [8] uses vorticity tubes to define vortices. Nitsche [9] asserts, "A vortex is commonly associated with the rotational motion of fluid around a common centerline. It is defined by the vorticity in the fluid, which measures the rate of local fluid rotation." An immediate contradiction to these definitions is that the Blasius boundary layer where the vorticity is large near the wall, but no rotational/swirling motion (considered as a vortex) is observed, as the vorticity cannot distinguish a vortical region from a shear layer region. In addition, the maximum vorticity does not necessarily represent the center of the vortex. Robinson [10] pointed out that the association between regions of strong vorticity and actual vortices can be rather weak in the turbulent boundary layer, especially in the near wall region. Wang *et al.*, [11] also found that vorticity magnitude will be reduced when vorticity lines enter the vortex region and vorticity magnitude inside the vortex region is much smaller than the surrounding area, especially near the solid wall in a flat plate boundary layer, for most three-dimensional vortices like Λ-shaped vortices.

Another possible candidate for vortex definition is the one based on closed or spiraling streamlines [12]. Robinson *et al.*, [13] claim, "A vortex exists when instantaneous streamlines mapped onto a plane normal to the vortex core exhibit a roughly circular or spiral pattern, when viewed from a reference frame moving with the center of the vortex core". Although it seems intuitive, Lugt [12] pointed out that "the definition and identification of a vortex in unsteady motions is difficult since streamlines and pathlines are not invariant with respect to Galilean and rotational transformations. Recirculated streamline patterns at a certain instant in time do not necessarily represent vortex motions in which fluid particles are moving around a common axis. Thus, instantaneous streamline patterns do not provide enough information to be used for the definition of a vortex."

Due to the essential requirement for visualizing vortical structures and their evolution in turbulence, several vortex identification criteria have been developed, including λ_2-criterion [14], Q-criterion [15], λ_{ci}-criterion [16], and $\lambda_{\mathrm{cr}}/\lambda_{\mathrm{ci}}$-criterion [17], *etc*. Nevertheless, these methods still fail to provide a rigorous definition of vortices. Moreover, these methods require proper thresholds. It is difficult to determine which threshold is proper, since different thresholds will indicate different vortical structures. For example, even if the same DNS data on the late boundary layer transition is employed, "vortex breakdown" will be exposed for some large threshold in Q-criterion while no "vortex breakdown" can be found for some smaller threshold. This will directly influence one's understanding and explanation on the mechanism of turbulence generation, *i.e.* turbulence is caused by "vortex breakdown" or not caused by "vortex breakdown". Recently, a new vortex identification method called Ω-method is given by the proposer, based on the idea that a vortex is a connected area where the vorticity overtakes the deformation [18]. The vorticiy represents the fluid's intention to rotate but deformation would resist rotation. Ω-method possesses several advantages, such as normalized from 0 to 1, no need for a case-related threshold, clear physical meaning and capability to capture both strong and weak vortices simultaneously. However, it is still not the ideal answer to the question of the mathematical definition of vortex, owing to some limitations such as the introduction of an artificial parameter ε and the incapability to identify the swirl axis and its orientation. Kolář [19] formulated a triple decomposition from which the residual vorticity can be obtained after the extraction of an effective pure shearing motion and represents a direct measure of the pure rigid-body rotation of a fluid element. However, the triple decomposition is not unique, so a so-called basic reference frame must be first determined. Searching for the basic reference frame results in an expensive optimization problem for every point in the flow field, which limits the applicability of the method. Kolář *et al*., [20-21] also introduced the concepts of the maximum corotation and the average corotation of line segments near a point and apply these methods for vortex identification. However, the so-called maximum-corotation method suffers from the unstable

CHAPTER 2

Liutex and Its Calculation and Galilean Invariance

Yiqian Wang[1,*], Yisheng Gao[2] and Chaoqun Liu[3]

[1]*School of Mathematical Science, Soochow University, Suzhou 215006, China*
[2]*College of Aerospace Engineering, Nanjing University of Aeronautics and Astronautics, Nanjing 210016, China*
[3]*Department of Mathematics, University of Texas at Arlington, Arlington, Texas 76019, USA*

Abstract: The Liutex (previously known Rortex) method introduces a vortex vector field to mathematically and systematically describe vortices in flow fields. In this study, the previous calculation procedures of Liutex which includes a two-step reference coordinate rotation is revisited first. An explicit formula to calculate Liutex is then derived and the physical intuition and efficiency improvement brought by this formula are discussed. It is estimated that the computation time of Liutex vector from velocity gradient field can be reduced by 36.6% compared with that of the previous method. Besides, the Galilean invariance widely accepted as a preliminary check for a successful vortex identification method is discussed for Liutex vector.

Keywords: Angular velocity, Coherent structures, Galilean invariance, Liutex, Vortex identification, Velocity gradient tensor.

.

INTRODUCTION

Despite that turbulence is often considered random, instantaneous organized structures, or coherent structures exist in turbulence and play a significant role in turbulent momentum transport [1-2]. Two typical coherent structures found in near-wall turbulence are the hairpin vortex and low-speed streaks. Theordorsen [3], back in 1952, proposed a conceptual model of “horseshoe” or “hairpin” vortex to describe the regeneration cycle of turbulence. Actually, these hairpin shaped vortices are ubiquitously found in wall turbulence both from numerical simulations and experiments. Adrian [4] has stipulated that hairpins may autogenerate to form hairpin vortex packets which are presumed to be the prevalent coherent structures in wall bounded turbulence. In a transitional boundary layer flow, the development from the Λ-vortex to the hairpin vortex was carefully studied by Wang *et al*. [5] and its preponderance and statistical importance in turbulence and transition was further investigated by Eitel-Amor [6]. The second type of coherent structure considered

***Corresponding author Yiqian Wang:** School of Mathematical Science, Soochow University, Suzhou 215006, China; Tel: +1-15950504139; E-mail: yiqianw@sina.com

Chaoqun Liu and Yisheng Gao (Eds.)

here is the near-wall streaks of alternating high and low streamwise momentum fluids which were first reported by Kline *et al*. [7] based on flow visualization in the viscous sublayer using hydrogen bubbles. Thereafter, substantial attention had been drawn to the streaks with the surrounding staggered quasi-streamwise vortices and the dynamics of the nonlinear self-sustain cycle concerning the streak instability that leads to the formation of quasi-longitudinal vortices was proposed [8]. Clearly, both the hairpins and the streaks are related to the notion of vortex, which has a clear physical intuition but hardly a mathematical definition. Δ, $\boldsymbol{\lambda_{ci}}$, $\boldsymbol{Q}$ and $\boldsymbol{\Omega}$ methods [9-12] which are classified into velocity-gradient-based Eulerian scalar vortex identification methods have been proved to be able to capture the vortical rotational strength to some extent. To give a more precise and unambiguous definition of a vortex, a vector field which includes information of both the direction and the magnitude named Liutex (previously named Rortex) [13-14] has been introduced recently. Then Gao and Liu [15] have improved the calculation method of Liutex by pointing out that the local rotational axis is actually the real eigenvector of the velocity gradient tensor provided that the other two corresponding eigenvalues are complex conjugates which serves as the sufficient and the necessary condition of local fluid rotation.

However, an explicit formula for Liutex vector has not been reached, making the derivation of governing equation more difficult and the appreciation of the physical meaning ambiguous. In the present study, a careful derivation of such an explicit formula is given after a revisit of the Liutex vector calculation procedure. Thereafter, the physical meaning and efficiency improvement of calculating the Liutex vector from this formula are discussed and also the Galilean invariance of Liutex is reassured according to the explicit formula.

REVISIT OF THE LIUTEX VECTOR DEFINITION

The computation of Liutex vector includes the following three steps.

1) Obtain the directional information of Liutex.

Calculate the eigenvalues of the 3×3 matrix $\nabla\vec{\boldsymbol{v}}$ (velocity gradient tensor) in the original xyz-frame. If all the three eigenvalues are real, there is no fluid rotation. Thus, the Liutex vector equals to zero. If $\nabla\vec{\boldsymbol{v}}$ has two complex conjugated eigenvalues and one real eigenvalue, the corresponding real unit eigenvector $\vec{t}_r$ is the local rotational axis and thus Liutex direction. Then, make a coordinate rotation (Q rotation) that rotates the original z-axis to the local rotational axis $\vec{t}_r$ and obtain the new velocity gradient tensor $\nabla\vec{\boldsymbol{V}}_{\boldsymbol{Q}}$ in the resulting XYZ_Q frame by $\nabla\vec{\boldsymbol{V}}_{\boldsymbol{Q}} = \boldsymbol{Q}\nabla\vec{v}\boldsymbol{Q}^{\mathrm{T}}$.

2) Obtain the magnitude of Liutex.

After the Q rotation, $\nabla\vec{\boldsymbol{V}}_{\boldsymbol{Q}}$ in the XYZ_Q reference frame has the form of:

$$\nabla\vec{\boldsymbol{V}}_{\boldsymbol{Q}} = \begin{bmatrix} \frac{\partial U_Q}{\partial X_Q} & \frac{\partial U_Q}{\partial Y_Q} & 0 \\ \frac{\partial V_Q}{\partial X_Q} & \frac{\partial V_Q}{\partial Y_Q} & 0 \\ \frac{\partial W_Q}{\partial X_Q} & \frac{\partial W_Q}{\partial Y_Q} & \frac{\partial W_Q}{\partial Z_Q} \end{bmatrix} \quad \textbf{(1)}$$

Another rotation (P rotation) is then applied to rotate the reference frame around the Z_O-axis and the velocity gradient tensor $\nabla\vec{\boldsymbol{V}}_P$ in the resulting XYZ_P coordinate can be expressed as:

$$\nabla\vec{\boldsymbol{V}}_P = \boldsymbol{P}\nabla\vec{\boldsymbol{V}}_Q\boldsymbol{P}^{-1} \quad \textbf{(2)}$$

where

$$\boldsymbol{P} = \begin{bmatrix} cos\theta & sin\theta & 0 \\ -sin\theta & cos\theta & 0 \\ 0 & 0 & 1 \end{bmatrix} \quad \textbf{(3)}$$

The resulting $\partial U_P/\partial Y_P$ under rotation angle θ is the angular velocity at this azimuth angle θ, and could be obtained as:

$$\frac{\partial U_P}{\partial Y_P}|_\theta = \alpha\sin(2\theta + \varphi) - \beta \quad \textbf{(4)}$$

with α and β determined by the elements of $\nabla\vec{\boldsymbol{V}}_Q$:

$$\alpha = \frac{1}{2}\sqrt{\left(\frac{\partial V_Q}{\partial Y_Q} - \frac{\partial U_Q}{\partial X_Q}\right)^2 + \left(\frac{\partial V_Q}{\partial X_Q} + \frac{\partial U_Q}{\partial Y_Q}\right)^2} \quad \textbf{(5)}$$

$$\beta = \frac{1}{2}\left(\frac{\partial V_Q}{\partial X_Q} - \frac{\partial U_Q}{\partial Y_Q}\right) \quad \textbf{(6)}$$

CHAPTER 3

New Omega Vortex Identification Method Based on Determined Epsilon

Xiangrui Dong[1,2], Yisheng Gao[3] and Chaoqun Liu[2,*]

[1]*Institute of Energy and Power Engineering, University of Shanghai for Science and Technology, Shanghai 200093, China*

[2]*Department of Mathematics, University of Texas at Arlington, Arlington, Texas 76019, USA*

[3]*College of Aerospace Engineering, Nanjing University of Aeronautics and Astronautics, Nanjing 210016, China*

Abstract: A new Omega (Ω) method with ε determination is introduced to represent the ratio of vorticity square over the sum of vorticity squared and deformation squared, for vortex identification. the advantages of the new Ω method can be summarized as follows: (1) Ω, as a ratio of the vorticity squared over the sum of the vorticity squared and deformation squared, is a normalized and case-independent function which satisfies $\Omega \in [0,1]$; (2) Compared with the other vortex visualization methods, which require a wide threshold to capture the vortex structures, Ω can always be set as 0.52 to capture vortex for different cases and time steps; (3) ε is defined as a function without any adjustment on its coefficient for all cases; (4) The Ω method can capture both strong and weak vortices simultaneously. In addition, Ω is quite robust with no obvious change in vortex visualization.

Keywords: Case-independent, Deformation, Omega method,Vortex identification, Vorticity.

INTRODUCTION

The definition and identification of vortex has been a longstanding issue in fluid dynamics. Robinson *et al.* [1] proposed a rather accurate definition: a vortex exists when instantaneous streamlines mapped onto a plane normal to the vortex core exhibit a roughly circular or spiral pattern, when viewed from a reference frame moving with the center of the vortex core. Several vortex identification methods based on the velocity gradient tensor $\nabla \boldsymbol{V}$ have been widely used to investigate the

***Corresponding author Chaoqun Liu:** Department of Mathematics, University of Texas at Arlington, Arlington, Texas 76019, USA; Tel: +1-8172725151; Fax: +1-8172725802; E-mail: cliu@uta.edu

Chaoqun Liu and Yisheng Gao (Eds)

vortex structures in turbulent flows. Perry and Chong [2] suggested a $\tilde{\Delta}$-method with an idea that the vortices exist where eigenvalues of velocity gradient tensor $\nabla \boldsymbol{V}$ are complex, which implies the streamline pattern is spiral or closed viewed from a reference frame moving with the point. This method was further developed by Zhou *et al.* [3] and called λ_{ci}. They suggested employing iso-surfaces of imaginary part of the complex eigenvalue to capture vortices. A famous Q-criterion was introduced by Hunt *et al.* [4], in which an eddy is defined as the region with positive second invariant Q of the velocity gradient tensor. Another well-known scheme is the λ_2 method, introduced by Jeong and Hussain [5]. They suggested the usage of second eigenvalue of the symmetric tensor $\mathbf{S}^2 + \boldsymbol{\Omega}^2$ trying to capture the pressure minimum in a plane normal to the vortex axis. All these methods have achieved some success. However, a threshold is required case by case and time by time, which means different thresholds will lead to different vortex structures. Zhang *et al.* [6] discussed various vortex identification methods in their study, and pointed out that those identification methods are too sensitive to the chosen threshold, making them inadequate for the quantitative analysis of the vortex. The improper thresholds may be able to only capture strong vortices but lose weak ones.

DEFINITION OF A VORTEX BY NEW OMEGA METHOD

A new vortex identification method, called Omega (Ω), first proposed by Liu *et al*. [7], appears to overcome the above-mentioned weaknesses. Recently, Zhang *et al*. [6] applied this new Ω method into the analysis of the reversible pump turbine and indicated that this new omega method is quite suitable for the analysis of complex flow of hydro-turbines, especially for the unsteady flow cases. Tao *et al.* [8] also utilized Ω to investigate the wake flow from moving bodies in their study, and they pointed out that comparing to other vortex identification methods, the new Ω method has a clear physical meaning and vortex is formed when the vorticity is strong but deformation is weak. Ω method was also used by other researchers [9-11] to compare with the existing vortex identification methods. Thus, the definition of Ω is introduced in the following section.

A parameter Ω is introduced to represent the ratio of vorticity over the whole velocity gradient inside a vortex core. According to Helmholtz velocity decomposition, the velocity gradient tensor $\nabla \boldsymbol{V}$ can be decomposed into a symmetric tensor and an anti-symmetric tensor,

$$\nabla \boldsymbol{V} = \frac{1}{2}(\nabla \boldsymbol{V} + \nabla \boldsymbol{V}^T) + \frac{1}{2}(\nabla \boldsymbol{V} - \nabla \boldsymbol{V}^T) = \mathbf{A} + \mathbf{B} \qquad \textbf{(1)}$$

where $\mathbf{A}$ is symmetric part which represents deformation and $\mathbf{B}$ is anti-symmetric part which is related to the whole vorticity. Now the ratio Ω is defined as a ratio of vorticity squared over the sum of vorticity squared and deformation squared, which shows vortex is formed when the vorticity is strong but deformation is weak,

$$\Omega = \frac{\|\mathbf{B}\|_F^2}{\|\mathbf{A}\|_F^2 + \|\mathbf{B}\|_F^2} = \frac{b}{a+b} \quad \textbf{(2)}$$

where $\|\cdot\|_F$ is the Frobenius norm. a and b is given below,

$$a = \mathrm{trace}(\mathbf{A}^T\mathbf{A}) = \sum_{i=1}^{3}\sum_{j=1}^{3}\left(\mathbf{A}_{ij}^2\right) \quad \textbf{(3)}$$

$$b = \mathrm{trace}(\mathbf{B}^T\mathbf{B}) = \sum_{i=1}^{3}\sum_{j=1}^{3}\left(\mathbf{B}_{ij}^2\right) \quad \textbf{(4)}$$

There is no doubt that $\Omega \in [0, 1]$, since both a and b are not negative. In fact vortex is a measurement of fluid stiffness. If $\Omega = 1$, fluid will behave as a solid rotation. If $\Omega = 0.5$, fluid has strong shear without rotation. Fluid is different from solid and is a mixture of vorticity and deformation. $\Omega > 0.5$ represents the region where vorticity overtakes deformation ($b > a$), which is defined as vortex. Although Ω is non-dimensional and satisfies $\Omega \in [0, 1]$, some serious noises (clouds) may appear inside the flow domain if both term a and b in equation (2) are in close proximity to zero due to the systematic computational errors. These noises can be reduced or even removed by introducing a proper positive number, ε, in the denominator of Ω. Therefore, in application, we pick,

$$\Omega = \frac{b}{a+b+\varepsilon} \quad \textbf{(5)}$$

ε is introduced in fact to remove noises caused by the consequence of division by zero. Apparently, as a positive number, ε is dependent upon the dimension of the physical variables and needs to be adjusted to a proper number case by case and time by time. A linear correlation is found between ε and the maximum of $b - a$. The Epsilon ε is defined as a function of $(b - a)_{\max}$, which is a fixed parameter at each time step in each case. In this study, ε is proposed as follows,

$$\varepsilon = 0.001 * (b - a)_{\max} = 0.002 * Q_{\max} \quad \textbf{(6)}$$

It should be noted that equation (6) is an empirical formula based on a large number of test results from different cases. The term $(b - a)_{\max}$ represents the maximum of the difference of vorticity squared and deformation squared, and is easy to obtain as a fixed number at each time step in a certain case. The adjustment of ε in any

CHAPTER 4

Stability Analysis on Shear Flow and Vortices in Late Boundary Layer Transition

Jie Tang*

Department of Mathematics, University of Texas at Arlington, Arlington, Texas 76019, USA

Abstract: Turbulence is still an unsolved scientific problem, which has been regarded as "the most important unsolved problem of classical physics". Liu proposed a new mechanism about turbulence generation and sustenance after decades of research on turbulence and transition. One of them is the transitional flow instability. Liu believes that inside the flow field, shear (dominant in laminar) is unstable while rotation (dominant in turbulence) is relatively stable. This inherent property of flow creates the trend that non-rotational vorticity must transfer to rotational vorticity and causes the flow transition. To verify this new idea, this chapter analyzed the linear stability on two-dimensional shear flow and quasi-rotational flow. Chebyshev collocation spectral method is applied to solve Orr–Sommerfeld equation. Several typical parallel shear flows are tested as the basic-state flows in the equation. The instability of shear flow is demonstrated by the existence of positive eigenvalues associated with disturbance modes (eigenfunctions), *i.e.* the growth of these linear modes. Quasi-rotation flow is considered under cylindrical coordinates. An eigenvalue perturbation equation is derived to study the stability problem with symmetric flows. Shifted Chebyshev polynomial with Gauss collocation points is used to solve the equation. To investigate the stability of vortices in flow transition, a ring-like vortex and a leg-like vortex over time from our Direct Numerical Simulation (DNS) data are tracked. The result shows that, with the development over time, both ring-like vortex and leg-like vortex become more stable as Omega becomes close to 1.

Keywords: Shear flow, Stability analysis, Transition, Turbulence, Vortices.

INTRODUCTION

A Short History Review of Research on Flow Transition and Turbulence Generation

In fluid flow, the process of a laminar flow becoming turbulent is a fundamental scientific phenomenon, known as laminar-turbulent transition. Laminar flow describes the fluid flows in parallel layers, with no disruption between the layers [1]. Turbulent flow is characterized by eddies or small packets of fluid particles

***Corresponding author Jie Tang:** Department of Mathematics, University of Texas at Arlington, Arlington, Texas 76019, USA; Tel: 8179081296; E-mail: jietanguta@gmail.com

Chaoqun Liu and Yisheng Gao (Eds.)

which result in lateral mixing [2]. Laminar-turbulent transition is an extraordinarily complicated process which at present is still far from fully understood. Nevertheless, as the result of many decades of intensive research, classical comprehensive theories of physical mechanisms of the transition phenomenon have been proposed [3-5].

Boundary layer is a very important concept in transition theory. It is a thin layer of viscous fluid close to the solid surface of a wall in contact with a moving stream [6]. The flow velocity varies from zero at the wall up to approximate free stream velocity at the boundary. The fundamental concept of the boundary layer was suggested by L. Prandtl [7] in 1904. Modern research on fluid transition is most often studied in the context of boundary layers due to their ubiquity in real flows and their importance in many fluid-dynamic processes [8].

In a thin boundary layer, the velocity gradient is significant, and consequently the viscous shear stresses defined by is large, where μ is the dynamic viscosity, $u = u(y)$ describes the profile of the boundary layer longitudinal velocity component, y is the normal-to-wall direction. In other words, in a thin boundary layer, laminar flow is dominant with shear layers.

$$\tau = \mu \frac{du}{dy} \tag{1.1}$$

Computation of the boundary layer parameters is based on the solution of equations obtained from the Navier–Stokes equations for viscous fluid motion. Navier-Stokes equations describe the conservation of mass, momentum, and energy.

For boundary-layer flows, two main classes of transition are known [9-11] depending on the character of environmental disturbances. The first of them is usually observed when environmental disturbances are rather small. It is regarded as natural transition and has fundamental and practical importance in problems involving moving vehicles in air and water. The second class of transition, usually called bypass, is observed when high enough levels of environmental perturbations are present.

Classical theory on natural transition can be described by four stages: receptivity, linear instability, non-linear growth and vortex breakdown as shown in Fig. (**1-1**) [5].

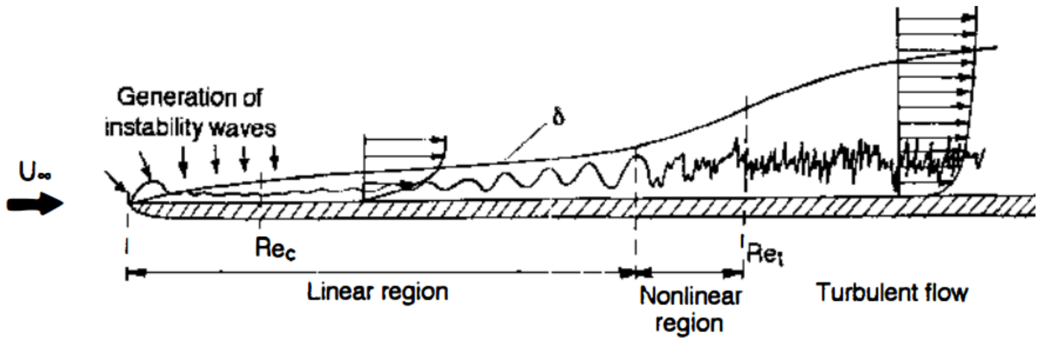

Fig. (1-1). Qualitative sketch of the process of turbulence onset in a boundary layer. δ is the thickness of the boundary layer, Re represents the Reynolds number and U_∞ is the income free stream **[5]**.

The initial stage of the natural transition process is known as the receptivity phase and consists of the transformation of environmental disturbances into small perturbations (*i.e.* instability waves, usually called Tollmien-Schlichting waves) within the boundary layer. This aspect of the transition process was clearly formulated for the first time by Morkovin [10] in 1968. Many experimental and theoretical work of this process appeared in the 1970s [11-16]. Details of the subsequent rapid development of investigations on receptivity can be found in a number of books and review papers [17-21].

The second stage of transition corresponds to the linearly propagation of small-amplitude instability waves in the boundary. This stage is described by linear hydrodynamic stability theory, also called linear stability theory. Tollmien [22] started the research on linear stability theory in 1929. In the following century, it becomes the most developed branch of the transition problem with a lot of research achievements for two-dimensional and three-dimensional flows. For example, Schlichting [23], Lin [24], Herbert [25] and many others.

When the growth of linear instability waves reaches considerable values, the flow enters a phase of three-dimensional nonlinear growth, then the turbulent flow formed (so-called vortex breakdown). They are the last two stages. Although the region of nonlinear growth has been studied for more than half century, there are still many questions unanswered [26-31]. For example, the mechanism of vortices generation and deformation, the formation of turbulence and turbulence coherent structure.

CHAPTER 5

POD and DMD Analysis in Late Flow Transition with Omega Method

Sita Charkrit and Chaoqun Liu*

Department of Mathematics, University of Texas at Arlington, Arlington, Texas 76019, USA

Abstract: In this paper, the proper orthogonal decomposition (POD) and dynamic mode decomposition (DMD) are applied to analyze the 3D late transitional flow on the flat plate obtained from direct numerical simulation (DNS). POD is used to find the most persistent spatial structures while DMD is used to find single frequency modes. The Omesga method is applied as a vortex identification to visualize vortices with isosurfaces $\Omega = 0.52$. The results in POD and DMD are discussed and compared to show the same and different features such as shapes, amplitudes and time evolutions.

Keywords: Dynamic mode decomposition, Identification method, Modal decomposition, Late flow transition, Omega method, Proper orthogonal decomposition.

INTRODUCTION

In the study of fluid flow structure in computation fluid dynamics (CFD), the modal decomposition is a useful tool to extract the whole structure into coherent structures in different features such as energy content, mode shape, amplitude and frequency since a complex flow structure often consists of a combination of coherent structure. The two popular modal decomposition methods, *i.e.*, the proper orthogonal decomposition (POD) and dynamic mode decomposition (DMD), are presented in this paper. The POD and DMD have been widely applied to explore the complex flow fields since they can be used to decouple the spatial and temporal applications. These two methods help in further understanding of fundamental fluid processes since they can examine the dominant and coherent structures in fluid flows.

The POD is one of the most widely used techniques to analyze fluid flows. There are two versions of POD technique. The original POD, proposed by Lumley [1] in

***Corresponding author Chaoqun Liu:** Department of Mathematics, University of Texas at Arlington, Arlington, Texas 76019, USA; Tel: +1-8172725151; Fax: +1-8172725802; E-mail: cliu@uta.edu;

Chaoqun Liu and Yisheng Gao (Eds.)

1967, is used to investigate the turbulent flow. The other version is called snapshot POD, which was introduced by Sirovich [2] in 1987. The snapshot POD is applied in order to optimize the computation. In POD, the flow structure is decomposed into orthogonal mode ranking by their kinetic energy content. In recent years, there have been many applications about POD in many fields of fluid dynamics. For examples, POD was used to study the turbulent pipe flow [3, 4]. In some studies [5, 6], POD was applied to identify turbulent discontinuous and nonlinear flows. A mixing layer downstream on a thick splitter plate obtain form DNS was analyzed by POD in a study [7]. The flow structure in transition stage has been analyzed by POD. For example, POD was applied to analyze coherent structures in pipe flow [8, 9] and a transitional boundary layer with and without control [10]. POD was also used to investigate asymmetric structures of flow on the flat plate [11]. The vortex structure in MVG wake was examined [12]. The entropy generation in a laminar separation boundary layer was analyzed by POD [13].

The other popular decomposition method used in this paper is DMD, which was first introduced by Schmid [14] in 2010 to extract the dynamic features by finding the relationship between each time step. Each coherent structure has a single feature in temporal mode. This method relates to Koopman operator explained in the paper of Rowley [15]. Many researchers applied DMD and compared both POD and DMD to analyze the flows in CFD. For instance, Premaratne and Hu [16] studied turbine wake characteristics by DMD. Alina and Navon [17] used DMD in shallow water and a swirling flow problem. Mohan and Gaitondey [18] worked on analysis of deep dynamic stall on a plunging airfoil by DMD. Both methods were compared in terms of identification of multi-dominant coherent structures and high-order harmonics buried in fluid flow in a study [19]. The POD and DMD on LES of subsonic jets were presented in a study [20].

The purpose of this work is to apply POD and DMD to investigate the complex flow on the flat plate in late transition stage obtained from direct numerical simulation (DNS) and to better understand its three-dimensional structure. Moreover, the vortex identification method called the omega method is introduced to visualize the vortex structures of spatial modes. This paper is organized as follows. In section 2, the detail of DNS data used in this paper is introduced. In section 3, the concept of Omega method is described. In section 4, descriptions of POD and DMD are explained. In addition, the analyses in both POD and DMD are discussed and compared in section 4.

CASE SETUP AND CODE VALIDATION

The case and code validation are presented in studies [21, 22]. The computational domain is demonstrated in Figs. (**1** and **2**). The grid level is 1920 x 128 x 241, representing the number of grids in streamwise (x), spanwise (y), and wall normal (z) directions. The grid is stretched in the normal direction and uniform in the streamwise and spanwise directions. The length of the first grid interval in the normal direction at the entrance is found to be 0.43 in wall units (Z+ = 0.43). The flow parameters, including Mach number, Reynolds number, etc. are listed in Table **1**. The DNS code, DNSUTA, has been validated by NASA Langley and UTA researchers carefully to make sure the DNS results are correct. For more detail about case setup and code validation, see [21, 22].

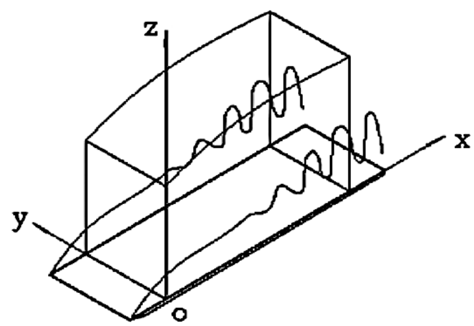

Fig. (1). Computation domain.

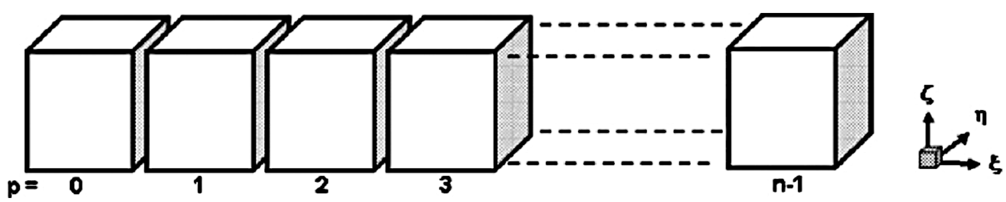

Fig. (2). Domain decomposition along the streamwise direction in the computational space.

Table 1. DNS parameters.

M_∞	Re	x_{in}	Lx	Ly	Lz_{in}
0.5	1000	$300.79\delta_{in}$	$798.03\delta_{in}$	$22\delta_{in}$	$40\delta_{in}$

CHAPTER 6

Comparison of Liutex and Eigenvalue-based Vortex Identification Criteria for Compressible Flows

Yisheng Gao[1] and Chaoqun Liu[2,*]

[1]*College of Aerospace Engineering, Nanjing University of Aeronautics and Astronautics, Nanjing 210016, China*

[2]*Department of Mathematics, University of Texas at Arlington, Arlington, Texas 76019, USA*

Abstract: Currently, the Q criterion, the Δ criterion and the λ_{ci} criterion are representative among the most widely used vortex identification criteria. These criteria can be categorized as eigenvalue-based criteria since they are exclusively determined by the eigenvalues or invariants of the velocity gradient tensor. However, these criteria are not always satisfactory and suffer from several defects, such as inadequacy of identifying the rotational axis and contamination by shearing. Recently, a novel concept of Liutex (previously named Rortex), including the scalar, vector and tensor form, was proposed to overcome the issues associated with the eigenvalue-based criteria. In the present paper, the comparison of Liutex and two eigenvalue-based criteria, namely the λ_{ci} criterion and the Q_D criterion, a modification of the Q criterion, is performed to assess these methods for compressible flows. According to the analysis of the deviatoric part of the velocity gradient tensor, all the scalar, vector and tensor forms of Liutex are valid for compressible flows without any modification, while two eigenvalue-based criteria, though applicable to compressible flows, will tend to be severely contaminated by shearing as for incompressible flows. Vortical structures induced by supersonic microramp vortex generator (MVG) at Mach 2.5 are examined to confirm the validity and superiority of Liutex for compressible flows.

Keywords: Compressible flows, Liutex/Rortex, Vortex identification, Vortex structures, Turbulence.

INTRODUCTION

Vortical structures, or formally referred to as coherent structures [1-3], are widely regarded as one of the most principal features of transitional and turbulent flows and serve a crucial role in turbulence generation and sustenance. During the last

***Corresponding author Chaoqun Liu:** Department of Mathematics, University of Texas at Arlington, Arlington, Texas 76019, USA; Tel: +1-8172725151; Fax: +1-8172725802; E-mail: cliu@uta.edu

several decades, some typical elementary structures, such as hairpin vortices [4-7], vortex braids [8-9] and quasi-streamwise vortices [1, 10-11] *etc.*, have been identified and intensively studied. Unfortunately, despite the ubiquity and signify-cance of such spatially and temporally coherent vortical motions in transitional and turbulent flows, an unambiguous and rigorous definition of the vortex is yet to be achieved (without doubt, the concept of coherent structures is also somewhat ambiguous). The lack of a well-accepted definition has been perceived as one of the chief obstacles hindering the thorough understanding of vortical structures and the mechanism of turbulence generation and sustenance [12-13].

The classic vortex dynamics generally associate the vortex with the vorticity since the vorticity is mathematically mathewell-defined (the curl of the velocity vector). For example, Saffman [14] regards a vortex as a “finite volume of vorticity immersed in irrotational fluid.” Nitsche [15] suggests that “a vortex is commonly associated with the rotational motion of fluid around a common centerline. It is defined by the vorticity in the fluid, which measures the rate of local fluid rotation.” Wu *et al*. [16] declares that “a vortex is a connected region with high concentration of vorticity compared with its surrounding”. However, the usage of vorticity-based methods is not always satisfactory, especially for turbulence flows. The prominent issue is that the vorticity cannot distinguish between a region with real vortical motion and a shear layer region. A typical example is the Blasius boundary layer where the magnitude of the vorticity is relatively large in the near-wall regions, but no real rotational motion will be observed. In addition, the vorticity can be somewhat misaligned with the direction of vortical structures [17]. It is not uncommon that the vorticity vector angle will be significantly larger than the local inclination of the vortex structure over almost the entire length of the quasi-streamwise vortex in the channel flow [18]. And the association between regions of strong vorticity and actual vortices can be rather weak in the turbulent boundary layer, especially in the near wall region [19]. In fact, it has been found by Wang *et al*. [20] that in the near-wall regions, the magnitude of the vorticity will be dramatically reduced along vorticity lines entering the vortex core.

To overcome the issues associated with vorticity-based methods for the identification and visualization of vortex structures, numerous vortex identification methods, including Eulerian non-local methods, Eulerian local region-type methods, Eulerian local line-type methods and Lagrangian methods have been proposed during the last three decades [21]. Most of the currently popular vortex identification criteria belong to Eulerian local region-type methods. Most of these criteria are exclusively determined by the eigenvalues or invariants of the velocity gradient tensor and thereby can be categorized as eigenvalue-based criteria. For example, the Q criterion [22] defines vortices as the regions where the vorticity magnitude prevails over the strain-rate magnitude. The Δ criterion [23-25] identifies the region where the velocity gradient tensor has complex eigenvalues by the discriminant of the characteristic equation. The λ_{ci} criterion [18] is an extension of the Δ criterion, which uses the (positive) imaginary part of the complex eigenvalue to determine the swirling strength. The λ_2 criterion [26] is a dynamical definition and based on the second-largest eigenvalue of $\boldsymbol{S}^2 + \boldsymbol{\Omega}^2$ ($\boldsymbol{S}$ and $\boldsymbol{\Omega}$ represent the symmetric and the antisymmetric parts of the velocity gradient tensor, respectively. Also, it should be noted that λ_2 can be exclusively determined by the eigenvalues only if the eigenvectors of the velocity gradient tensor are orthonormal). These methods can discriminate against shear layers, offering more detectable vortex structures than vorticity-based methods. Nevertheless, there exist several shortcomings of the eigenvalue-based criteria. One is the user-specified threshold. On one hand, the threshold is case-dependent and cannot be determined beforehand. On the other hand, no one can confirm if a threshold is appropriate or not, because different thresholds will present different vortical structures [27]. Therefore, the educed structures obtained from these criteria should be interpreted with care. As a remedy, relative values can be employed to avoid the usage of case-related thresholds, and one such example is the Omega method [28-30]. The Omega method (Ω) is originated from an idea that the vortex is a region where the vorticity overtakes the deformation and Ω is defined as a ratio of vorticity tensor norm squared over the sum of vorticity tensor norm squared and deformation tensor norm squared. Thus, the Omega method is robust to moderate threshold change and capable to capture both strong and weak vortices simultaneously. Another obvious drawback is the inadequacy of identifying the swirl axis or orientation. The existing eigenvalue-based criteria are scalar-valued criteria, which means that only iso-surfaces will be obtained, and no rotational axis can be identified by these criteria. In addition, eigenvalue-based criteria are prone to contamination by shearing [31-33]. The problem of contamination by shear motivates Kolář [34] to propose a triple decomposition from which the residual vorticity can be obtained after the extraction of an effective pure shearing motion and represents a direct and accurate measure of the pure rigid-body rotation of a fluid element. However, a basic reference frame (BRF) should be first determined and searching for BRF in 3D cases is very challenging, which severely limits the applicability of the triple decomposition. The extensive overview of the currently available vortex identification methods has been provided by several review papers [21, 35-36].

CHAPTER 7

Observation of Coherent Structures of Low Reynolds Number Turbulent Boundary Layer by DNS and Experiment

Panpan Yan[1,2], Chaoqun Liu[2,*], Yanang Guo[3] and Xiaoshu Cai[3]

[1]*Shenyang Aircraft Design and Research Institute, Aviation Industry of China, Shenyang 110035, China*

[2]*Department of Mathematics, University of Texas at Arlington, Arlington, Texas 76019, USA*

[3]*Institute of Particle and Two-phase Flow Measurement, University of Shanghai for Science and Technology, Shanghai 200093, China*

Abstract: An elaborate direct numerical simulation (DNS) for late boundary layer transition has been conducted. The DNS results are qualitatively compared with a new Lagrangian property experimental technique named the moving single-frame and long-exposure (MSFLE) imaging method to obtain a deeper understanding on the coherent structures of a transitional and turbulent boundary layer at low Reynolds number. Multilevel vortex structures are clearly observed by both experiment and DNS. This study found that there are multilevel co-rotating vortices, showing how energy is transported from the main flow to the bottom of the boundary layer and how the streaks or white-black strips are formed. The results also show that the lower level vortices cannot simply be produced by the upper-level vortex inducement. There are multilevel hairpin vortex ejections and sweeps inside the boundary layer of the transitional and low Reynolds number turbulent flows. The ejections and sweeps are much stronger around the hairpin legs and necks than those in the ring area. This clearly shows that the ring-like vortices are the production of the strong vortex neck rotation. In conjunction with ejections and sweeps, a lot of strong shear layers are produced. Because fluid cannot tolerate the strong shear, the shear layer must turn to rotation and form many vortices. This would help reveal the mechanism of multilevel vortices and turbulence generation. Although the upper-level vortices could be larger than the lower ones, the lower level vortices sometimes have the same size as the neighboring upper-level vortices. The vortex cascade and large vortex breakdown are not observed by either DNS or experiment.

Keywords: DNS, Ejection and sweep, Hairpin vortices, Multilevel vortices, experiment, Turbulent boundary layer.

***Corresponding author Chaoqun Liu:** Department of Mathematics, University of Texas at Arlington, Arlington, Texas 76019, USA; Tel: +1-8172725151; Fax: +1-8172725802; E-mail: cliu@uta.edu

Chaoqun Liu and Yisheng Gao (Eds.)

INTRODUCTION

Wall-bounded turbulent flow is a fundamental scientific topic and has received a lot of attention for over a century due to its importance to both scientific research and many industrial applications such as transition control and drag reduction in aerospace engineering [1, 2]. Many efforts have been made for turbulent boundary layer flow [3-5]. However, the mechanism of wall-bounded turbulent flow still remains a puzzle. Nearly four decades ago, Falco [6] gave a well-known visualization of a low Reynolds number turbulent boundary layer that illustrates several known types of coherent structures. Theodorsen [7] had identified the horseshoe vortex in wall-bounded turbulent flow by experimental observation. Robinson [8] believed that the coherent structure is responsible for the production and dissipation of turbulence in a boundary layer, and the study of turbulence structures is of fundamental importance to understand and control the turbulent boundary layer. Kline *et al*. [9] found that the long streamwise streaks of hydrogen bubbles in the near-wall region by experiment and that the spanwise spacing of these streaks were about 100 wall units. They believed that the instability of these streaks plays a vital role in turbulence generation. Working with Kline, Robinson [10] gave a summary of the structures. He observed that quasi-streamwise vortices are located close to the wall, arches or horseshoe vortices in the wake region, and there is a mixture of quasi-streamwise vortices and arches in the logarithmic layer. Liu *et al*. [11-13], Rist *et al*. [14], and Wu and Moin [15] obtained transitional and low Reynolds number turbulent flow with a forest of hairpin vortices through DNS while Eitel-Amor found that the hairpin vortex structures are not a feature in fully developed turbulence [38]. Scaling theories coupled with the notion of coherently organized motions were first proposed by Townsend [16, 17] and advanced by Perry and Chong [18]. They gave a model of individual hairpin vortices scattered randomly in the flow and found that the vortices are statistically independent of each other. They imagined the wall layer as a forest of single layer hairpin vortices which can be modeled with simplified shapes in a hierarchy of scales above the wall. Yan *et al*. [19] found that the hairpin vortex is a combination of the Λ-vortex roots and vortex rings. Λ-vortex roots and vortex rings are formed separately and independently, and the mechanism of the Λ-vortex self-deformation to hairpin vortex does not exist. Liu *et al.* [20, 21] believed that turbulence is an inherent property of fluid flow, although the external disturbance is needed. The nature of turbulence generation is that fluids, away from the wall, cannot tolerate the shear, and shear must transfer to rotation. Therefore, we believe shear layer instability is the mother of turbulence. However, physics of turbulence is very complex and a number of articles have given a variety of theories [22-27]. Adrian [28] believed hairpins could be auto-generated to form packets that populate a significant fraction of the boundary layer, and he addressed the important role of hairpin vortex ejections and sweeps. Marusic's review paper [3] mentioned that there is still a dichotomy on whether the hairpin vortex exists or not. Schoppa and Hussain [29] thought complete hairpin vortices do not exist in wall bounded turbulence. Therefore, more work must be conducted to get a deep understanding about the vortex structure of the low Reynolds number turbulent boundary layer.

A new Lagrangian property experiment technique, which is named as the moving single-frame and long-exposure (MSFLE) imaging method, is proposed for measuring the coherent structure in a turbulent boundary layer. Meanwhile, a high order direct numerical simulation with nearly 60 million grid points with 400,000 time steps is carried out in order to get a deep understanding of the coherent structure for the low Reynolds number turbulent boundary layer flow.

This chapter is organized in the following way. In Section 2, the DNS case setup and validation and the experiment setup are described. Section 3 provides the comparison of the DNS results with the experiment and describes our new DNS observations. Finally, some conclusions are presented in Section 4.

CASE SET UP

DNS Case Setup and Code Validation

Fig. (**1**) shows the computational domain where *x*, *y*, *z* represent the streamwise, spanwise and wall-normal directions respectively. There are 1920×128×241 grid points in the computation domain. The points are distributed uniformly in the streamwise and spanwise directions and stretched in the wall normal direction to ensure the grid has enough resolution to capture all small length scales. The first grid interval is set to 0.43 in wall units (z^+=0.43) in the normal direction. As shown in Fig. (**1b**), the whole domain is decomposed in the *x*-direction to implement parallel computation by using the Message Passing Interface (MPI) technique. Table I gives the details of the flow conditions including Mach number, Reynolds number, *etc*. Here δ_{in} is the inflow displacement thickness, and other parameters are non-dimensionalized by δ_{in} as reference length. L_x and L_y are the length of computational domain in the x and y directions, and $L_{z_{in}}$ is the height of the inlet. x_{in} is the distance between the leading edge and inlet. T_w and T_∞ represent the wall temperature and freestream temperature. The Reynolds number of the inlet is defined as $Re = \rho_\infty U_\infty \delta_{in} / \mu_\infty$.

CHAPTER 8

Direct Numerical Simulation of Incompressible Flow in a Channel with Rib Structures

Ting Yu, Duo Wang, Heng Li, Hongyi Xu*

Aeronautics and Astronautics Department, Fudan University, Shanghai, PR China

Abstract: This **c**hapter applied the state-of-the-art flow simulation method, *i.e.* the Direct Numerical Simulation (DNS), and strongly coupled the DNS with the heat-transfer governing equation to solve the thermal turbulence in both 2-dimensional (2D) and 3-dimensional (3D) channels with the rib tabulator structures. An innovative approach was applied to the simulations. The surface roughness effects of the cooling vane were directly tackled by including the roughness geometry in the DNS and applying the immersed-boundary method to handle the geometry complexities due to the roughness. Two inlet conditions, namely the uniform flow and full-developed turbulence, were applied at the inflow surface of the channel. Half height of the channel was used as the scale length. The Prandtl (Pr) number was set at Pr = 0.7. Five Reynolds (Re) number of 1000, 2500, 5000, 7500 and 10000 were calculated in the 2D cases and the Reynolds numbers of 2500 and 5000 were applied in 3D cases where a periodical condition was applied in the span-wise direction. Additionally, Reynolds number of 10000 was set in the case with roughened surface. The stream-wise velocity, turbulence intensity, and the Nusselt (Nu) number were analyzed. Results in the 2D and 3D cases presented a significant difference on flow structure. At the same time, with increasing Reynolds number, the length of recirculation zone and the enhancement of heat transfer showed a decreasing trend.

Keywords: Direct Numerical Simulation, Heat Transfer, Rib Tabulator, Roughness, Rortex.

INTRODUCTION

Surface structures, such as pin-fins, ribs and dimples, are effective cooling methods in modern aero-engine design. These structures are commonly used to enhance heat exchange by increasing the heat-exchange surfaces and the turbulence level in flow.

***Corresponding author Hongyi Xu:** Aeronautics and Astronautics Department, Fudan University, Shanghai, PR China; Tel: 86-021-55665062; Email: hongyi_xu@fudan.edu.cn

Chaoqun Liu and Yisheng Gao (Eds.)

The rib tabulator is one of the important structures applied in aero-engine components, for example, the combustion ducts and the internal cooling channel of turbine blade. Therefore, it is important to study the flow around a rib and to analyze its effects on the flow field and closely-related heat transfer process. As well known, the flow separation occurs in front of a rib and then reattachment can be found at the bottom wall after rib. Many researches have been conducted to investigate the interactions of these structures with the strongly-coupled flow and heat transfer effects.

The experiments from Eaton *et al*. [1], Chun *et al*. [2], and Liu *et al*. [3] showed the strong unsteadiness of these flow structures. Bergeles and Athanassiadis [4] found that the structures included the combination of complex phenomena, such as flow separation and reattachment. Liu *et al*. [5] provided their experiment results about the flow over a rib, which tried to elucidate the unsteady behaviors of the separation and reattachment over a 2D square rib.

As the computational capabilities grew, more numerical results of flow over the rib were given. Leonardi *et al*. [6] presented the periodic flow in channel with square ribs, the relationship between the flow structure and the ratio of rib height to gap of two ribs was studied. LES method was applied by Cui *et al*. [7], which focused on two types of flows between the ribs. Matsubara *et al*. [8] and Miura *et al*. [9] simulated the flow structure and heat transfer of 3D rib with different Reynolds numbers and aspect ratios.

The current chapter numerically analyzed the flow and heat transfer processes in both 2D and 3D single-rib geometries. Ten cases were investigated including seven 2D cases and three 3D cases. The Reynold numbers (Re) of 2500, 5000 and 7500 were applied in the 2D cases, and the Re of 2500 and 5000 were applied in the 3D cases. Fully-developed turbulent inlet conditions were used in the case with Re=2500. Additionally, most previous work focused on the smooth boundary wall. Since these studies were not able to reflect the effects of the roughness, a 2D case with roughened boundary surfaces was simulated in this study. This case had six dis-symmetric ribs. The Reynolds number of 10000 was applied. Fully-developed turbulent inlet condition was used. X-ray scanning technologies were applied to obtain the geometric contours of the roughness on the cooling-vane surface. An immersed boundary (IB) method coupled with the adaptive mesh refinement technology was implemented to tackle the extremely complex geometries of the surface roughness [10]. In all cases, Prandtl number (Pr) was fixed at 0.7 in these studies to represent air flow. The state-of-the-art simulation method in fluid mechanics, namely Direct Numerical Simulation (DNS), was applied to obtain the flow solution, and multi-grid method was applied to increase the solution efficiency. In order to capture the turbulence and the associated vortical structure, a new vortex identification method was applied, namely, newly defined Rortex proposed by Liu *et al*. [10].

The data are useful and helpful in pushing the nowadays frontiers in each of these relevant science fields, such as the fluid mechanics, heat transfer as well as computations. Also, the database will help transforming the design and manufacture of the turbine blade from the current one based on engineering experiments and empirical data to the future one intelligently-guided by reliable simulation databank.

MATHEMATICAL-PHYSICAL MODELS AND METHODS

Governing Equations

The mathematical models included the conservations of mass, momentum and energy, which are written in the non-dimensional form under Cartesian coordinators:

$$\frac{\partial \bar{u}_j}{\partial x_j} = 0 \quad \textbf{(1)}$$

$$\frac{\partial \bar{u}_j}{\partial t} + \frac{\partial \bar{u}_j \bar{u}_i}{\partial x_j} = -\frac{\partial p}{\partial x_j} + \frac{1}{\mathrm{Re}}\frac{\partial}{\partial x_j}\left(\frac{\partial \bar{u}_i}{\partial x_j} + \frac{\partial \bar{u}_j}{\partial x_i}\right) \quad \textbf{(2)}$$

$$\frac{\partial \theta}{\partial t} + \frac{\partial \bar{u}_j \theta}{\partial x_j} = \frac{1}{RePr}\frac{\partial^2 \theta}{\partial x_j \partial x_j} + \frac{Ec}{Re}\frac{1}{2}\left(\frac{\partial \bar{u}_i}{\partial x_j} + \frac{\partial \bar{u}_j}{\partial x_i}\right)\left(\frac{\partial \bar{u}_i}{\partial x_j} + \frac{\partial \bar{u}_j}{\partial x_i}\right) \quad \textbf{(3)}$$

where the subscripts $i, j, k = 1,2,3$ represented the three spatial directions x, y, z, with x being the stream-wise and y, z being the cross-streamwise directions; the repeated subscripts followed the Einstein summation; $\bar{u}_j$ and θ are the non-dimension forms of velocities and the temperature, respectively, and p is the static pressure. The criterion numbers of Re, Pr and Ec are defined as $Re = \rho U h/\mu$, $Pr = \mu C_p/k$ and $Ec = U^2/C_p(Th - Tc)$ with ρ, μ, C_p being the fluid density, molecular viscosity and specific heat capacity, U being the fluid incoming velocity, $Th\ and\ Tc$ being the hot(wall) and cool(incoming) temperatures, respectively, and h being the height of rib as seen in Fig. (**2**).

CHAPTER 9

Vortex and Flow Structure inside Hydroturbines

Yuning Zhang [1*], Yuning Zhang [2, 3,]**

[1]*Key Laboratory of Power Station Energy Transfer Conversion and System (Ministry of Education), School of Energy, Power and Mechanical Engineering, North China Electric Power University, Beijing, China*
[2]*College of Mechanical and Transportation Engineering, China University of Petroleum-Beijing, Beijing 102249, China*
[3]*Beijing Key Laboratory of Process Fluid Filtration and Separation, China University of Petroleum-Beijing, Beijing 102249, China*

Abstract: In this chapter, various kinds of vortex in the hydroturbines are briefly introduced with a focus on the swirling vortex rope in Francis turbine and the vortex in the vaneless space of the reversible pump turbine. The vortex induced pressure fluctuation and vibrations are initially demonstrated based on the on-site measurement in the prototype power stations. Then, influences of the vortex in the upstream on the flow status in the downstream are discussed. Finally, detailed characteristics of the swirling vortex in the draft tube section of the hydroturbines are demonstrated based on the plenty of examples together with the aid of a quantitative swirl number analysis.

Keywords: Hydroturbines, Pressure fluctuations, Vibrations, Vortex, Vortex rope.

A SUMMARY OF TYPES OF VORTEX IN HYDROTURBINES

There are various kinds of hydroturbines including Francis turbine, reversible pump turbine, Kaplan turbine, Pelton turbine etc. For a complete review of the flow-induced vortex in hydroturbines together with the vortex identification methods and their applications in hydroturbines, readers are referred to Zhang *et al*. [1]. For reference books relating with the associated pressure fluctuations and vibrations in hydroturbines, readers are referred to Wu et al. [2] and Dörfler *et al*. [3]. Fig. (**2**) of Chen *et al*. [4] shows the Francis turbine of Three Gorges hydro power station, which was the largest hydroturbines (in terms of the electricity generation capacity)

***Corresponding author Yuning Zhang:** Key Laboratory of Power Station Energy Transfer Conversion and System (Ministry of Education), School of Energy, Power and Mechanical Engineering, North China Electric Power University, Beijing, China; Tel: 86 (0)1061773958; E-mail: y.zhang@ncepu.edu.cn

Chaoqun Liu and Yisheng Gao (Eds.)

of the given type in the world when it was commissioned. In the above figure, the detailed components of the aforementioned hydroturbines are also shown. Basically speaking, the fluid passing components of a typical Francis turbine include the spiral casing, the stationary guide vane, the wicket gate (also named as the adjustable guide vane, with the function of the water flux control), runner (also named as impeller), draft tube (including cone and elbow sections respectively). For other types of the hydroturbines, the basic structures and principles are quite similar. In the present chapter, two paramount types of the hydroturbines are discussed: the aforementioned Francis turbine and the reversible (Francis type) pump turbines of a pumped hydro energy storage power plant.

For different kinds of hydroturbines, the dominant types of vortex are quite different. For example, for the Francis turbine, the dominant vortex is usually the swirling vortex rope in the draft tube (referring to the figure 13 of Chen *et al*. [4]). When the turbine is operated in the partial loads (off-design conditions), this kind of vortex is quite strong with significant rotating momentum. Meanwhile, prominent pressure fluctuation will be also generated by the swirling vortex rope with the propagation to the upstream or the downstream also possibly leading to the vibrations of the whole unit. Generally speaking, the rotational speed of this kind of vortex is rather slow and is far less than the rotational speed of the runner. Other prominent vortex also exists in the channel of runner (termed as the channel vortex).

For the reversible pump turbine, as shown in figure 16 of Zhang *et al*. [5], the dominant vortex is the vortex shown in the vaneless space between the wicket gate and the runner (also named as the impeller). For more details about the reversible pump turbine, readers are referred to Zhang *et al*. [5]. In the vaneless space, as shown in figure 12 of Hasmatuchi *et al*. [6], there are prominent backflows during the low discharge mode. Comparing with the best design point (BEP), the flow status is much distorted in the low discharge working conditions, leading to the strong channel blockage of the flow. For the reversible pump turbine, the vortex rope in the draft tube also exists but is no longer the primary source of the vortex as those shown in the Francis turbine.

For the Kaplan turbine, the tip vortex between the runner and the hub is very significant, leading to serious damage on the fluid components. Generally speaking, because the tip is quite small according to the design (for the enhancement of the efficiency), cavitation usually occurs near the tip. Hence, as shown in figure 14 of Motycak *et al*. [7], the tip leakage vortex is often accompanied by the cavitation bubbles. Because the force and micro-jet generated by the bubble final collapse are quite prominent, serious damage could be observed on the runner edges.

Other types of vortex also include the inter-blade vortex in the runner, the Kármán vortex in the wake flow of the vanes and the cavitating vortex.

The relationships between the vortex and the turbulence could be illustrated as follows. On the one hand, the vortex phenomenon could induce the generations of the turbulence together with associated structures. For example, during the rotating stall status in the reversible pump turbine, the vortex generated in the impeller channels could block the fluid passing through the component. With the increment of the fluid distortion, a strong turbulence flow will be finally demonstrated with prominent pressure fluctuations. On the other hand, the existing turbulence will lead to the intensive generations of the vortex. For example, in the low load condition, the turbulence will be induced inside the guide vane channels due to the large incidence angle. Then, many small vortex will appear especially near the pressure side of the vanes.

THE EFFECTS OF VORTEX ON PRESSURE FLUCTUATION

In this section, various kinds of negative effects of the vortex on the hydroturbine performances will be introduced including the pressure fluctuation together with its characteristic frequency.

Fig. (**2**) by Zhang *et al*. [8] shows the non-dimensional peak-to-peak values of pressure fluctuation versus load variations (from 25.41% to 96.82% of the full load) at four monitoring points (referring to the ref. [8] for the positions). The identified three zones could be summarized as follows:

Zone 1: This zone corresponds to the conditions of the low partial load. The pressure fluctuation is mainly generated by the vortex flow in the vaneless space. Fig. (**4**) of Zhang *et al*. [8] further shows the cascade plot of frequency spectrums measured at the vaneless space. The dominant frequency is $9f_n$ (also termed as blade passing frequency, with f_n representing the impeller rotational frequency), which is generated by vortex induced by the rotating impeller.

Zone 2: This zone corresponds to the conditions of the medium partial load. The pressure fluctuation is mainly generated by the swirling vortex rope in the draft tube cone section. Figure 5 of Zhang et al. [8] further shows the cascade plot of frequency spectrums measured at the draft tube cone section. The dominant frequency of this kind of vortex is less than f_n, which is generated by the vortex induced by the swirling vortex rope.

CHAPTER 10

A Comparative Study of Compressible Turbulent Flows Between Thermally and Calorically Perfect Gases

Xiaoping Chen*

National-Provincial Joint Engineering Laboratory for Fluid Transmission System Technology, Zhejiang Sci-Tech University, Hangzhou, Zhejiang 310018, China

Abstract: In this chapter, direct numerical simulations (DNSs) of compressible turbulent flows for thermally perfect gas (TPG) and calorically perfect gas (CPG), including two wall temperature of 298.15K (low temperature condition) and 596.30K (high temperature condition), are performed to investigate the influence of a gas model on the turbulent statistics and flow structures. The results show that the influence of TPG is negligible and remarkable for low and high-temperature conditions, respectively. Many of the statistical characteristics used to express low-temperature conditions for CPG still can be applied to high-temperature conditions for TPG. The smaller the influence of the gas model on the mean and fluctuating velocity, the stronger the Reynolds analogy. The static temperature for TPG is smaller than that for CPG, whereas an inverse trend is found for turbulent and root square mean Mach numbers. Omega could capture both strong and weak vortices simultaneously for compressible flow, even TPG, which is difficult from Q. Compared to the results of CPG, the vortex structure becomes smaller, sharper and more chaotic considering TPG.

Keywords: Calorically perfect gas, Compressible flow, Direct numerical simulation, Thermally perfect gas, Vortex structure.

INTRODUCTION

Compressible flow has critical importance in gas dynamics and engineering application. The heat flux and frictional resistance in turbulent flow are obviously higher than that for laminar flow. For compressible turbulent flows, the near wall

***Corresponding author Xiaoping Chen:** National-Provincial Joint Engineering Laboratory for Fluid Transmission System Technology, Zhejiang Sci-Tech University, Hangzhou, Zhejiang, 310018, China; Tel+86 18626878196; E-mail: chenxp@zstu.edu.cn

Chaoqun Liu and Yisheng Gao (Eds.)

temperature may be higher than 500K. Here, it will be changed the thermodynamic environment, which means that the calorically perfect gas (CPG) no longer appropriate and the thermally perfect gas (TPG) [1] should be considered. Therefore, assumed to be TPG, the behavior of turbulent statistical characteristics and flow structures in compressible turbulent flow urgently needs to be investigated.

Direct numerical simulation (DNS) does not involve any modeling errors and solves the Navier-Stokes equations directly [2], which is a powerful tool to simulate the turbulent flows, including channel flows [3-10], boundary layers [11-15], compression ramps [16, 17], and blunt cones [18-20]. A large number of DNS study is reported to investigate the statistical characteristics in the compressible turbulent flows, such as strong Reynolds analogy (SRA) and Morkovin's hypothesis. The Morkovin hypothesis [21] denotes that, when the Mach number isn't very large, the relationship of turbulent statistical characteristics between incompressible and compressible flows can be connected by mean variations of fluid properties. Huang *et al.* [5] investigated compressibility effects based on the DNS data of compressible turbulent channel flow performed by Coleman *et al.* [4]. Lechner *et al.* [6] and Foysi *et al.* [7] studied compressible effects and turbulence scaling in the compressible turbulent channel flow. The differences in turbulence statistics near both the adiabatic and isothermal walls were reported by Mamano et al [8] and Morinishi et al [9]. In addition, to some extent, the energy equation can be explained by SRA-a relationship between velocity and temperature fluctuations. Morkovin [21] firstly proposed SRA in 1963. Then, researches proposed several modified SRA, such as ESRA was introduced by Cebeci *et al.* [22], GSRA was introduced by Gaviglio [23], RSRA was introduced by Rubesin [24], HSRA was introduced by Huang *et al.* [5] and GHSRA was introduced by Duan *et al.* [25]. So far, many studies of supersonic turbulent boundary layer flows have been performed to check the validity of SRA and Morkovin's hypothesis by the DNS data. For example, Duan and Martin [13, 14] assessed the influence of Mach number and wall temperatures on the SRA and Morkovin's hypothesis. Liang and Li [15] investigated many turbulent characteristics, such as Walz equation, mean and fluctuating velocity, compressibility effect and SRA

For the compressible turbulent flow, the behaviour of instantaneous vortex structures is also very important. Many criterions for identify turbulent structures have been introduced in many literatures, such as $\tilde{\Delta}$-criterion [26-27], Q-criterion [28], λ_2-criterion [29], λ_{ci}-criterion [30], the Ω criterion [31, 32], and Rortex [33]. Based on the DNS results of boundary layer, these criterions were evaluated by Sayadi *et al.* [34] and Pierce *et al.* [35]. They found that these criterion produce the same images as chosen the threshold of $10^{-3}\left(\partial u/\partial y\right)^2\Big|_w$. Coleman *et al.* [4] illustrated that near-wall streak in the stream-wise direction become more coherent as the Mach number increased. They also argued that the weakly compressible hypothesis modifies the near-wall structures little. Morinishi *et al.* [9] showed that the thermal wall boundary condition has very little effect on the near-wall streaks in semi-local units. For the supersonic boundary layers, Lagha *et al.* [36, 37] studied the influence of Mach number on the near-wall structure. Guo and Adams [38] illustrated that near-wall streak structures are larger than that of incompressible flow. Most previous studies have been carried out on calorically perfect gas (CPG), a good understanding is gained due to these works.

So far, many DNS results for TPG were performed based on DNS. Marxen *et al.* [39, 40] studied the effects of gas model on the stability of hypersonic boundary layer. In the hypersonic boundary layer, Jia and Cao [41] investigated the behavior of stability of flat plate under different variable specific heat. Recently, taking temporally evolving compressible turbulent flows as a research object, Chen *et al.* [42-46] not only performed several DNS, but also investigated the similarities and differences between TPG and CPG. However, the turbulent statistics and flow structures in compressible turbulent flows for TPG have not been studied clearly, especially for vortex structures, SRA and Morkovin's hypothesis.

In the present study, based on the DNS database, we focus on the behavior of turbulent statistical characteristics and flow structures in the compressible turbulent channel flow for TPG, and discuss how they depend on the wall temperature.

GOVERNING EQUATIONS

The governing equations are the time-dependent three-dimensional Navier-Stokes equations in non-dimensional form, which can be described as follows:

$$\frac{\partial \rho}{\partial t}+\frac{\partial}{\partial x_j}\left(\rho u_j\right)=0 \tag{1}$$

$$\frac{\partial\left(\rho u_i\right)}{\partial t}+\frac{\partial}{\partial x_j}\left(\rho u_i u_j+p\delta_{ij}-\frac{1}{\mathrm{Re}}\sigma_{ij}\right)=\rho f_i \tag{2}$$

$$\frac{\partial E}{\partial t}+\frac{\partial}{\partial x_j}\left[\left(E+p\right)u_j-\frac{1}{\mathrm{Re}}\left(u_i\sigma_{ij}+q_j\right)\right]=\rho f_i u_i \tag{3}$$

Current Developments in Mathematical Sciences, 2020, *Vol. 2*, 265-279

CHAPTER 11

The Experimental Study on Vortex Structures in Turbulent Boundary Layer at Low Reynolds Number

Yanang Guo, Xiaoshu Cai*, Wu Zhou, Lei Zhou and Xiangrui Dong

Institute of Particle and Two-phase Flow Measurement, College of Energy and Power Engineering, University of Shanghai for Science and Technology, Shanghai 200093, China

Abstract: Experiments with a moving single-frame and long-exposure (MSFLE) imaging method, which is a Lagrangian-type measurement, is carried out to study the vortex structures in a fully developed turbulent boundary layer at low Reynolds number on a flat plate. In order to give the process of the vortex generation and evolution, on the one hand, the measurement system moves at the substantially same velocity as the vortex structure; on the other hand, a long exposure time is selected for recording the paths of the particles. In the experiment, the vortex structure characteristics as well as the temporal-spatial development can be shown by the streamwise-normal (x-y)-plane and streamwise-spanwise (x-z)-plane images which are extracted from a fully developed turbulent boundary layer. The result shows that the interaction between high- and low-speed streaks induces the generation, deformation and 'breakdown' of the vortex structures, and badly influences the vortex evolution.

Keywords: Boundary layer, High- and low-speed streaks, Low Reynolds number, Moving single-frame and long-exposure time, Vortex structures, Vortex generation, Vortex evolution, Vortex breakdown, Turbulent.

INTRODUCTION

The coherent structures play a significant role in the friction drag, heat and mass transfer, and the turbulence kinetic energy of turbulent boundary layer. However, the vortex structure is dominant and badly affects the generation and evolution of other coherent structures. Thus, the study on vortex structures is the starting point of the turbulence research.

In 1952, Theodorsen [1] proposed the horseshoe vortex as the basic structures in

***Corresponding author Xiaoshu Cai:** Institute of Particle and Two-phase Flow Measurement, College of Energy and Power Engineering, University of Shanghai for Science and Technology, Shanghai 200093, China; Tel: +86-21-55275059; E-mail: usst_caixs@163.com

Chaoqun Liu and Yisheng Gao (Eds.)

wall-bounded turbulent flow. Kline *et al.* [2] analyzed a turbulent boundary layer flow field by hydrogen bubble. The high- and low-speed spots and the long streamwise streaks of hydrogen bubble were found in the near-wall region. In addition, they used dye to be the tracer for flow visualization and suggested that bursting is an important factor for energy generation of turbulence. A visual study of a turbulent boundary layer flow was conducted by photographing the motions of small tracer particles ($d = 62 - 74\mu$m) using a stereoscopic medium-speed camera system moving with the flow by Brodkey *et al.* [3]. They found that the ejections could be a consequence of low-speed fluid being trapped between fingers of high-speed fluid. Head *et al.* [4] conducted an experiment by a smoke tunnel with a 45 degree light sheet to visualize the hairpin vortex in turbulent boundary layer flow. Adrian *et al.* [5-9] studied the structure of energy-containing turbulence in the outer region of a zero-pressure gradient boundary layer by using particle image velocimetry (PIV) to measure the instantaneous velocity fields in a streamwise-normal plane. They found that the hairpin vortices in the outer layer occur in streamwise-aligned structures and could form large scale packets. The experimental investigations by the hydrogen bubble technique were performed by Lian [10] to show the coherent structures of turbulent boundary layer. In their experiment, the streamwise- and normal-vortices were observed along the interface regions between high- and low-speed streaks, while, the transverse (spanwise) vortices were observed at the front of the high-speed regions. Lozanoduran *et al.* [11] and Zandonade *et al.* [12] pointed out that the coherent structures in turbulent boundary layer could be illustrated by the high- and low-speed streaks and the vortices. The generation of these high- and low-speed streaks is related to the ejection and sweep, while, the generation of the vortices is related to the shear layer. Gao *et al.* [13] proposed and implemented a moving tomographic particle image velocimetry method to measure temporal evolution of velocity fields in three-dimensional volumes and to track coherent structures within a turbulent boundary layer with $Re_\tau \approx 2410$.

Although the vortex structure in turbulent boundary layer has been widely studied, and people already have had some understandings on its structural characteristics, its mechanism is still not clear. To further study the essence of vortex structure in turbulent boundary layer, the dynamic evolution of vortex structure with time and space must be obtained. In this paper, the moving single-frame and long-exposure (MSFLE) imaging method is utilized to study the vortex structure in a fully developed turbulent boundary layer on the flat plate at low Reynolds number. The evolution process of the vortex structure as well as the interaction between streaks and vortices have been discussed.

EXPERIMENTAL METHODS

Moving Single-Frame and Long-Exposure (MSFLE)

For most imaging measurements, the camera is usually fixed without moving, such as PIV and single-frame and long-exposure (SFLE). Fig. (**1**) gives the schematic diagram of the SFLE imaging measurement. The principle of SFLE is introduced in the following.

Firstly, the tracer particles with good tracking property are interspersed in the flow field; then, these tracer particles are illuminated by a light sheet from the laser; finally, the scattered light of the particles can be received by the camera. It means that the trajectory of the particles can be recorded in a single frame image by setting a proper exposure time of the camera. The length of the path line represents the movement distance of the tracer particle during the exposure time, thus the velocity of the tracer particle *V*, can be obtained as:

$$V = \frac{S}{M\Delta t} \tag{1}$$

Where *S* is the total length of trajectory, *M* is magnification factor of lens and Δt is exposure time. Moreover, the direction of the particle velocity can be determined by two consecutive frames.

However, it would be failed to capture the process of the fast-moving vortex structure evolution if the camera is fixed. Here, the MSFLE imaging method, which is developed from the SFLE method, is utilized to show both of the temporal and spatial development of the vortex structure in a single frame image, without using vortex identification criteria or Galilean velocity decomposition. Compared to SFLE method, the advantage of MSFLE is that the camera can move in the measuring system so that vortex structures with the same speed as the camera can be captured. MSFLE is a Lagrangian-type measurement and it is easy to observe the evolution process of vortex structure intuitively.

CHAPTER 12

Experimental Studies on Coherent Structures in Jet Flows Using Single-Frame-Long-Exposure (SFLE) Imaging Method

Lei Zhou[1], Xiaoshu Cai[1,*], Wu Zhou[1] and Yiqian Wang[2]

[1]*Institute of Particle and Two-phase Flow Measurement, University of Shanghai for Science and Technology, Shanghai, China*

[2]*School of Mathematical Science, Soochow University, Suzhou, 215006, China*

Abstract: On the axisymmetric water jet experimental apparatus, the flow field structures in entrainment boundary layers are measured using Single Frame Long Exposure image method, in the range of Reynolds number (*Re*) 1849~2509. It is found that engulfing and nibbling entrainment model occur intermittently with time, in the region of L=2~3.5d streamwise and H=1~1.25d radial direction. It concludes that the occurrence probability of engulfing increases with Reynolds number when *Re*>1915, the influence of Reynolds number on the occurrence probability of this structures decreases when *Re*>2311; the occurrence frequency of this coherent structures obtained by fast Fourier transform is between 10 and 19Hz; special vortex structures were observed in the flow field during the occurrence of engulfing. The jet flow field is measured using Moving Single Frame Long Exposure image method in Lagrangian coordinate system, and it is found that the vortex structures generally exist near the interface of turbulent regions and non-turbulent regions.

Keywords: Entrainment layer, Jet, Move single frame long Exposure, Vortex structures, Single frame single exposure.

INTRODUCTION

The observation of alternating vortical structures on the two sides of a gaseous jet using stroboscopic cinematography by Brown [1] provided one of the earliest experimental evidence for the existence of coherent structures in jet flows. Davis, Fisher and Barratt [2] then reported that a chain of vortex rings exists in round turbulent jets and Beavers and Wilson [3] further confirmed that these vortical

***Corresponding author Xiaoshu Cai:** Institute of Particle and Two-phase Flow Measurement, University of Shanghai for Science and Technology, Shanghai, China; Tel: +86-21-55275059;
E-mail: usst_caixs@163.com

Chaoqun Liu and Yisheng Gao (Eds.)

structures are all located inside the shear layer region. Ever since, the investigation of coherent vortical structures in jet flows became a fundamental topic and received attentions from researchers. Westerweel, Hofmann, Fukushima and Hunt [4] studied the characteristics of the TNTI (turbulent/non-turbulent interface) in self-similarity jets by combining the techniques of PIV (Particle Image Velocimetry) and LIF (Laser Induced Fluorescence) and concluded that the profile of TNTI rapidly changes along the axial direction with violent mass, momentum and energy exchange. Gan [5-7] investigated the initial development of gaseous turbulent vortex rings by PIV and found that this coherent pattern forms around $x/d = 2.5$, where x is the axial coordinate and d is the nozzle diameter. Two-dimensional (2D) and three-dimensional (3D) PTV (Particle Tracking Velocimetry) are also applied to study the small-scale coherent structures in the developed region of turbulent jets. Moreover, Silva, Taveira and Borrell [8-12] classified the entrainment at the TNTI into engulfing (big-scale eddy motions) and nibbling small-scale eddy motions).

Undoubtedly, the coherent structures play an important role in the entrainment of turbulent jet flows. However, the generation and the development of these coherent structures, especially their relationship with the TNTI is still unclear. To study the dynamics as well as the physical mechanism of the entrainment in jet flows, a detailed analysis on the evolution of the coherent structures in a water jet flow by utilizing Single Frame Long Exposure (SFLE) and Moving Single Frame Long Exposure (MSFLE) developed in our group is carried out in this chapter.

EXPERIMENTAL METHODS

Single-Frame-Long-Exposure (SFLE) and Moving SFLE (MSFLE)

The trajectories of illuminated tracer particles are obtained by using a relatively long exposure time and a typical trajectory is shown in Fig. (**1a**). The length of the trajectory S can be regarded as the distance covered by the tracer particle during the exposure time Δt plus the diameter of the tracer particle D as shown in Fig. (**1b**). Given that Δt is sufficiently small, the velocity magnitude of the particle V can be estimated as

$$V = \frac{L}{K*\Delta t} = \frac{S-D}{K*\Delta t}$$

where K is the magnification factor of the camera lens, D is the diameter of the tracer particle and L is the distance covered by the tracer particle over Δt.

In the frame work of SFLE, the exposure time can be adjusted to accommodate to the targeting velocity, or Reynolds number based on the nozzle velocity V_j and the nozzle diameter d, *i.e.*, $Re = V_j d/\nu$, where ν is kinematic viscosity. In addition, information of the flow field with various resolution can be obtained by adjusting the magnification factor of the lens. Additional information of the moving direction can be acquired by the correlation between two consecutive snapshots or the SFME (Single-Frame-Multiple-Exposure) [13] technique. A schematic diagram of the SFLE is shown in Fig. (**2**). To study the coherent vortical structures from the instantaneous flow field, moving SFLE (MSFLE) is developed to remove the mean flow velocity by making the camera moving with a constant velocity in the axial direction. SFLE and MSFLE, which have the advantages of providing more intuitively vision of the flow field and more comprehensive information about the moving trajectories during an exposure time, thus are selected in this study to investigate the coherent vortical structures in a water submerged jet flow.

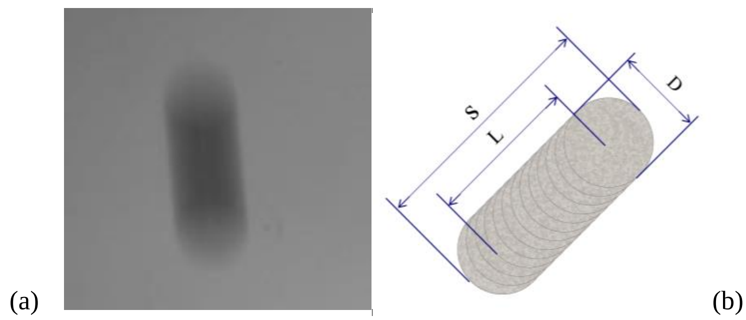

Fig. (1). (a) A typical trajectory by SFLE; **(b)** Sketch of a particle trajectory.

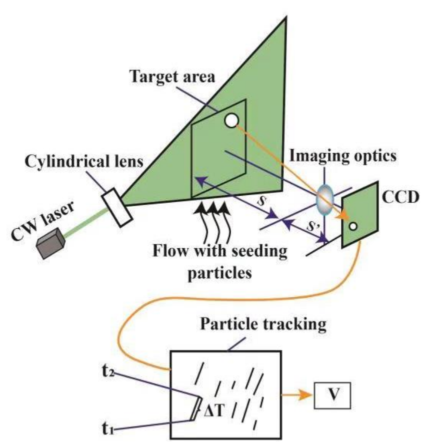

Fig. (2). A schematic diagram of SFLE.

Current Developments in Mathematical Sciences, 2020, *Vol. 2*, 293-311

CHAPTER 13

Hybrid Compact-WENO Scheme for the Interaction of Shock Wave and Boundary Layer

Jianming Liu[1,2] **and Chaoqun Liu**[2,*]

[1]*School of Mathematics and Statistics, Jiangsu Normal University, Xuzhou 221116, China*

[2]*Department of Mathematics, University of Texas at Arlington, Arlington, Texas 76019, USA*

Abstract: In this chapter, an introduction to hybrid Weighted Essentially non-oscillatory (WENO) method is given. The hybrid techniques including both central and compact finite difference schemes are introduced. The paper review about the driven mechanism of the high order finite scheme required for compressible flow with shock is presented. The detailed constructing processes of the compact and WENO schemes are given and the hybrid detector is introduced. Further, in particular, a series of examples in the field of the compressible flow are designed to illustrate the different methods.

Keywords: Navier-Stokes equation, High order finite difference scheme, Hybrid Compact-WENO, Shock wave and boundary layer interaction turbulence.

A SHORT REVIEW ON STUDY OF HIGH ORDER FINITE DIFFERENCE SCHEME FOR COMPRESSIBLE FLOWS

The compressible flow field is in general governed by the Navier-Stokes equations deduced from physical conservation law. Due to the complexity of the flow problems, if there is no high-order scheme, it is impossible to obtain exact results which can embody complex fluid structures with different scales. To date, there are many effective numerical discretization methods for compressible flow, such as finite difference method (FDM), finite volume method (FVM), discontinuous Galerkin method (DGM) [1], high-order flux reconstruction [2], Spectral volume/difference Method (SVM) [3], *etc*. The finite difference method is one of the main numerical methods of computational fluid dynamics (CFD) because of its simplicity and easy to achieve high precision with the longest history. In addition, it is one of the most mature, widely used, and the most effective method. Hence, in this chapter, we focus on the high-order FDM.

***Corresponding author Chaoqun Liu:** Department of Mathematics, University of Texas at Arlington, Arlington, Texas 76019, USA; Tel: +1-8172725151; Fax: +1-8172725802; E-mail: cliu@uta.edu

In the field of CFD, in general, we consider the scheme with at least third-order accuracy is high order. Since the 1990s, the research and application of high-order finite difference methods have begun to make substantial progress. In the present, the multi-scale complex flow such as simulating turbulence requires high-order numerical methods, which has become the consensus of the scientific community. Many scholars have developed a number of high-order numerical methods with advanced algorithms and good computational effects. Emerging advanced numerical methods include the ENO/WENO method [4-7], non-oscillatory containing no free parameter and dissipative (NND) scheme [8], group velocity control (GVC) scheme [9], compact scheme [10-12], *etc*. Among these numerical methods, the compact scheme only requires small number of grid points to get the high-order accuracy. The compact scheme had relatively small dissipation and gained a lot of favor in the field of direct numerical simulation (DNS) of turbulence flow [10-13]. The high-order central finite difference scheme is another kind of more effective method, which is straightforward and easy to implement and doesn't need to calculate the derivative performed by the compact scheme. Although compact scheme and high-order central scheme have obvious advantages in the simulation of multi-scale turbulent flow, it is hard to simulate the compressible flows with shock wave. On the other hand, to date, upwind or bias upwind high-order WENO scheme has achieved great success in capturing the shocks sharply. In the DNS of turbulence flow, the small length scale vortex is very important in the flow transition and turbulence process and thus very sensitive to any artificial numerical dissipation [11]. But the dissipation caused by WENO scheme is still harmful to the simulation of the flow transition of turbulent flow. Hence, in order to capture the shock waves sharply and resolve the small-scale turbulent flow simultaneously, a combination of compact or central and WENO schemes is desirable [11, 13-15].

Governing Equations

We consider the compressible Navier-Stokes equations in Cartesian tensor form as

$$\begin{gathered}\frac{\partial \rho}{\partial t}+\frac{\partial \rho u_j}{\partial x_j}=0,\\ \frac{\partial \rho u_i}{\partial t}+\frac{\partial \rho u_i u_j}{\partial x_j}=-\frac{\partial p}{\partial x_i}+\frac{\partial \tau_{ij}}{\partial x_j},\\ \frac{\partial E}{\partial t}+\frac{\partial u_i E}{\partial x_i}=-\frac{\partial p u_i}{\partial x_i}+\frac{\partial u_i \tau_{ij}}{\partial x_j}-\frac{\partial q_i}{\partial x_i},\end{gathered} \tag{1}$$

where

$$\tau_{ij} = \mu\left(\frac{\partial u_i}{\partial x_j} + \frac{\partial u_j}{\partial x_i} - \frac{2}{3}\frac{\partial u_k}{\partial x_k}\delta_{ij}\right),$$
$$q_i = -k\frac{\partial T}{\partial x_i}.$$

With the reference values of characteristic length L, the free stream speed U_∞, temperature T_∞, viscous coefficient μ_∞, density ρ_∞, and the pressure $\rho_\infty U_\infty^2$, the Navier-Stokes equation (1) can be non-dimensioned and the only changed terms are

$$\tau_{ij} = \frac{\mu}{Re}\left(\frac{\partial u_i}{\partial x_j} + \frac{\partial u_j}{\partial x_i} - \frac{2}{3}\frac{\partial u_k}{\partial x_k}\delta_{ij}\right),$$
$$q_i = -\frac{1}{Re(\gamma-1)PrMa_\infty^2}k\frac{\partial T}{\partial x_i}.$$

In order to illustrate the establishment of the finite difference scheme of Equation (1), we use the following simple scalar model equation as sample.

$$\frac{\partial u}{\partial t} + \frac{\partial f}{\partial x} = \mu\frac{\partial^2 u}{\partial x^2}. \tag{2}$$

The first derivative term in Equation (2) is used to simulate the convective term, and the second derivative term is used to simulate the viscous term in Navier-Stokes equation (1).

High-order Central Finite Difference Scheme

The main difficulty in the calculation of compressible fluid problems lies in the discretization of convective terms. To simulate the complex turbulence phenomena, it is significant to discretize the inviscid term by a high order method. In this study, we only consider the fourth/sixth- order approximation. The convect term $\frac{\partial f}{\partial x}$ at the grid point x_i can be approximated by

$$\left.\frac{\partial f}{\partial x}\right|_{x_i} = \frac{\hat{f}_{i+1/2} - \hat{f}_{i-1/2}}{\Delta x}. \tag{3}$$

The fourth order central difference scheme to approximate the face flux can be formulated as

$$\hat{f}_{i+1/2} = \frac{1}{12}(-f_{i-1} + 7f_i + 7f_{i+1} - f_{i+2}), \tag{4}$$

SUBJECT INDEX

A

B

C

Chaoqun Liu and Yisheng Gao (Eds.)

D

E

F

G

H

I

L

M

N

O

P

T

V

W

Z

Chaoqun Liu

Dr. Chaoqun Liu received both BS (1968) and MS (1981) degrees from Tsinghua University, Beijing, China and PhD (1989) degree from the University of Colorado at Denver, USA. He is currently a tenured and distinguished professor and the director of Center for Numerical Simulation and Modeling at the University of Texas at Arlington, Arlington, Texas, USA. He has worked on high order direct numerical simulation (DNS) and large eddy simulation (LES) for flow transition and turbulence for almost 30 years starting from 1989. As PI, he has been awarded by the NASA, US Air Force and US Navy with 50 federal research grants of over 5.7´106 US dollars in the United States.. He has published 11 professional books, 120 journal papers and 145 conference papers. He is the founder and major contributor of the third generation of vortex identification methods including the Omega, Liutex/Rortex, Liutex-Omega, Modified Liutex-Omega, Liutex Core Line methods, RS vorticity decomposition and R-NR velocity gradient decomposition.

Yisheng Gao

Dr. Yisheng Gao received his Bachelor of Engineering degree in aircraft design and engineering (2007), Master of Engineering degree in fluid mechanics (2009) and Ph. D. degree in fluid mechanics (2016) from the Nanjing University of Aeronautics and Astronautics University, China. His research is concerned with computational fluid dynamics, including direct numerical simulation and discrete adjoint methods.